

GUN TESTING
for the
GLASGOW SYNCHROTRONS
by

A.C.Robb
M.Eng. A.M.I.E.E.

An Account of an
Introductory Investigation

Submitted
as a Thesis for
the Degree of Doctor of Philosophy
in the
University of Glasgow

August
1955

ProQuest Number: 13838900

All rights reserved

INFORMATION TO ALL USERS

The quality of this reproduction is dependent upon the quality of the copy submitted.

In the unlikely event that the author did not send a complete manuscript and there are missing pages, these will be noted. Also, if material had to be removed, a note will indicate the deletion.



ProQuest 13838900

Published by ProQuest LLC (2019). Copyright of the Dissertation is held by the Author.

All rights reserved.

This work is protected against unauthorized copying under Title 17, United States Code
Microform Edition © ProQuest LLC.

ProQuest LLC.
789 East Eisenhower Parkway
P.O. Box 1346
Ann Arbor, MI 48106 – 1346

PREFACE

This study is concerned primarily with the performance of injection guns in electron synchrotrons. There are two such accelerators in the University of Glasgow, and the work described is concerned with both of them. The smaller, 30 MeV machine, which the author commissioned in Malvern and later installed in the Department of Natural Philosophy, is comparatively simple and uncomplicated by correction circuitry. Its performance therefore clearly illustrates many of the characteristics of the betatron injection process by means of which synchrotron acceleration is initiated. This process, and the problem of initial injection of electrons into the betatron orbit, is discussed in some detail at the beginning of the introduction. In a later part of the same section early experiments relating machine and gun performances are described. It was from these experiments that a project for testing guns independently of the accelerators in which they were to be used was first developed.

The project for independent gun testing initially involved building a suitable test unit, and this is described in detail in the second section of the following account. The third section is concerned with observational techniques, with calibration, and with the procedure for ageing guns to withstand high working voltages. The following section is initially concerned with the construction and electrical performance of the two types of electron gun used on the two Glasgow synchrotrons, and subsequently considers the relationship between gun and overall synchrotron performances. At this stage attention is concentrated particularly on the comparatively recently commissioned 300 MeV accelerator, in which initial injection requirements are particularly stringent.

A final section considers the nature of the information and experience derived from the work already described, and makes certain recommendations about possible future developments, in particular stressing the unsatisfactory characteristics of the present electron guns used on the 300 MeV machine.

.

It would not be fitting to conclude these prefatory remarks without acknowledging the valuable assistance

received in various stages of the work from colleagues in the Department; in particular from Mr J.M.Reid in collaboration during the commissioning of the smaller machine; and from Dr W.F.MacFarlane and other members of the 300 MeV synchrotron team, in provision of synchrotron test data and in collaboration to determine the behaviour of guns when operating in the accelerator. The author would also like to express special gratitude to Professor Philip I. Dee, and Professor Bernard Hague, who together made the submission of this thesis possible.

A. C. Robb

The Department of Natural Philosophy,
The University of Glasgow.

August 1955.

CONTENTS

	P
PREFACE	111
Contents	1
INTRODUCTION	
i) Programme	4
ii) Early work on the 30 MeV Synchrotron	20
iii) Betatron Characteristics of the 30 MeV Synchrotron	28
iv) Early Electron Gun Experiments on the 30 MeV Synchrotron	31
v) Implications of 30 MeV Synchrotron and Gun Tests	36
A GUN TESTING UNIT	
i) Basic Structure	38
ii) The Vacuum System	39
iii) Gun Supplies	43
iv) Monitoring Facilities	49
TEST TECHNIQUES	
i) Fluorescent Screens	52
ii) The Use of Fluorescent Screens	58
iii) The Probe Unit	61
iv) Uses of the Probe Unit	67

TEST TECHNIQUES (Continued)	p
v) High Voltage Calibration	68
vi) A Note on Ageing	76
GUN TESTING	
1) Gun Construction	79
ii) Electron Optics	84
iii) Beam Pattern Observations	94
iv) The General Correlation of Gun and Machine Performances	97
CONCLUSIONS	107
Alphabetical Reference List	111
Sequential Figure List	113

INTRODUCTION

1) Programme

Considerable experience has now been gained in Europe and America on the operation of electron synchrotrons. These machines almost invariably rely on betatron acceleration to raise the electrons to the relativistic velocity at which synchrotron acceleration becomes possible. The overall performance of such accelerators has been found to depend primarily on the number of electrons that can be usefully accelerated through the betatron process. This number is limited more acutely by the problems associated with initial introduction of the electrons into the accelerating chamber than by the later process of acceleration transfer, during which betatron acceleration diminishes and synchrotron acceleration begins. The preponderant importance of the initial injection process is

demonstrated by the fact that the transfer efficiency usually approximates closely to unity, and is many hundred or thousand times greater than the initial injection efficiency.

It is significant that this introductory process, despite its considerable importance, is still very incompletely understood. The inhomogeneities within the magnetic and electric fields at the time of injection are inordinately complicated, and vary widely from one machine to another; and, within one machine, from one setting to another. They are, moreover, partially obscure; so that only the most obvious may be isolated, accurately evaluated, and, where possible, eliminated: many others remain undetected or indeterminate. Under such conditions theoretical analysis is more useful as a broad pointer toward general relationships than as a precise tool for commissioning new machines: this work must remain very largely empirical.

To understand the injection problem it is therefore necessary both to refine approximate theory through empirical knowledge, and to confirm practical

experience by theoretical understanding. The work to be described in the following pages is primarily concerned with extending the range of empirical knowledge in the hope that a more complete theoretical understanding may subsequently be developed. The policy and programme adopted has been at once freely selected by the author and to some extent imposed upon him; for although there was a clear case for correlating machine performance with the characteristics of the electron gun used for the initial injection it was also desirable that the application of the available machines to nuclear physics experiments should be interfered with as little as possible. It became at once convenient and expedient to do much of the work away from and independent of the machines for which the guns were designed

.

Before describing the course of action decided upon, and the reason for adopting it, an outline may be given of the behaviour of electrons immediately after injection into a betatron. More detailed consideration of relevant injection theory will

follow subsequently, in a more appropriate context; in the final interpretation of results. The basic relationships outlined below were first collected together and presented by D.W.Kerst, who built the the first working betatron in 1940.¹

Betatron acceleration normally takes place in a machine of the type shown in Figure 1. The magnet is of laminated silicon steel construction and is usually a.c.-excited at mains frequency, or through a frequency-tripling transformer. Two separate flux-paths must be considered: a central path carrying a flux ϕ within the orbit; and a guide-field path carrying the orbit-constraining field H . Acceleration takes place in a rising magnetic field by virtue of the tangential electric field resulting from $\dot{\phi}$ which operates on the injected electrons. The stable orbit radius, r_0 , is determined by the relationship:

$$\dot{\phi} = 2\pi r_0^2 \dot{H},$$

¹ D.W.Kerst Physical Review 58 p841 1940
 Physical Review 60 p 47 1941

where:

ϕ is the total flux within the orbit

H is the flux density at the orbit

r_0 is the equilibrium orbit radius.

It may be noted that this equation is independent of the particle momentum, and that betatron acceleration is therefore possible for any particle velocity. It is also important to note that the peak central flux must be large; the mean flux density at the orbit always being half of that within it, unless the central flux-path is specially biassed.¹ The provision of this large alternating flux makes the betatron a costly and relatively inefficient machine to run; but the machine is nevertheless exceptionally valuable as a 'trans-relativistic' means for introducing electrons into

¹ Since it is the rate of change of the central flux that matters biassing of the central path can introduce economy in the iron requirements:

D.W.Kerst Physical Review 68 p233 1945

W.F.Westendorp Journal of Applied Physics 16 p657 1945

a synchrotron. At relativistic energies synchrotron acceleration is vastly more economical, and the betatron process needlessly extravagant. The application of the betatron principle beyond the threshold of relativistic energies has therefore been generally discontinued.

By preserving a proportional relationship between $\dot{\phi}$ and \dot{H} the equilibrium radius can be maintained approximately constant, and acceleration can be confined within a relatively narrow annulus. This geometry provides further opportunity for focussing the electrons within their orbit; a condition brought about if the guide-field, H , is made inversely proportional to r^n ; where n lies between zero and unity, and is usually between 0.25 and 0.75.

Because the electrons are injected into the accelerating chamber by means of a gun which is not transparent to electrons, injection must take place from a point some distance away from the equilibrium orbit. Post-injection oscillations will therefore occur about this orbit: they will be virtually undamped but will nevertheless diminish in amplitude through an essentially adiabatic change related to

the increase of particle energy and constraining field. It has been shown that the amplitude of the oscillations diminishes as the inverse square-root of the guide-field intensity, and that for radial and vertical oscillations about the equilibrium orbit the frequencies are:

$$f_{\text{radial}} = \frac{\omega}{2\pi} \sqrt{1-n}$$

$$f_{\text{vertical}} = \frac{\omega}{2\pi} \sqrt{n}$$

where ω is the angular velocity of the particle in the stable orbit.¹

It will be seen that if $n = 0.75$, $f_{\text{radial}} = \frac{\omega}{2\pi} \times \frac{1}{2}$ and $f_{\text{vertical}} = \frac{\omega}{2\pi} \times 0.867$. Electrons injected into such a field from a point radially displaced from the equilibrium orbit would pass the point of injection on the other side of the equilibrium orbit the first time round the annulus, but would probably strike the back of the gun on their second circuit.

1

Electrons injected above or below the equilibrium orbit would be more likely to be obstructed by the gun on the first turn, because the ratio between the angular velocities of vertical and orbital motion is more nearly unity. For this type of injection the desirable condition is that $n = 0.25$.

This elementary argument is based on the dynamics of a single electron in an annular field of uniform n -value. It also assumes complete azimuthal inhomogeneity; although in practice none of these requirements is satisfied and the complexity of the oscillatory motion is correspondingly increased. Kerst originally suggested that the energy with which the electrons are admitted to the accelerating chamber should be low; an argument based on the contention that if $\Delta E/E$, the ratio of the energy gained per turn to the injection energy, is large, the shrinkage of the post-injection oscillation will be more rapid. However, most of the inhomogeneity in the magnetic field is based on secondary fluxes created by eddy currents within components of the magnetic circuit. These inhomogeneities are in phase quadrature with the main field and therefore produce their greatest

effect as the main field passes through its zero value: they become zero at the peak value of the main field. In practice, then, Kerst's argument for low energy injection is usually outweighed by the serious effect of guide-field inhomogeneities near the flux zero - although such effects cannot completely explain many of the peculiarities evident in the injection process.¹

A more recent argument by Kerst suggests that the large electron current which leaves the gun and shortly afterward collides with it again or falls onto the accelerating chamber walls significantly alters the injection process; in particular, the rapid rise of this current at the front edge of the injection pulse, or its subsequent rapid collapse at the trailing edge briefly affecting both the electron oscillations and the equilibrium orbit radius.²

There is a good deal of evidence to show that some process of the kind Kerst describes does in fact take place. Direct evidence may be found in

¹ F.K.Goward Proceedings of the Physical Society
LXI p284 1948

² D.W.Kerst Physical Review 74 p503 1948

machines where the injection pulse is monitored as a current pulse to the accelerating chamber wall. In such machines, if the pulse is of simple enough shape to make the observation possible (the 30 MeV synchrotron to be discussed in the following pages satisfies this requirement), a small negative pulse may be seen superposed on the main one. This very small disturbance is the actual loss of current to the accelerating process and represents the initially accepted electrons. When the machine is working well this secondary pulse usually appears, for maximum output intensity, somewhere on the crest of the injection pulse. When, however, operation is critical, and the alignment is clearly less satisfactory than usual, it is frequently to be found riding on one of the steep edges of the main pulse.

A similar effect has been produced artificially by applying a current pulse at the moment of injection to a circular orbital coil.¹ Kerst outlined this

¹

G.D.Adams Review of Scientific Instruments
19,9 p607 1948

provision in his discussion of the effects of the initial large beam current on the finally accepted portion of it. Experience on the 30 MeV synchrotron already mentioned has, however, confirmed that this additional coil is only useful when a machine is unsatisfactorily aligned. The close correspondence between the pulse-edge acceptance condition and the unsatisfactory alignment which alone justifies use of the coil is striking, and there can be no doubt that displacement of the stable orbit by the overall injection current is a real and important phenomenon: whether it is normal rather than abnormal is less certain.

Although artificial and pulse-edge orbit shifting methods appear in these accounts only as abnormal aids to injection they do not confirm that the process involved is itself abnormal. Pulse-edge acceptance has been observed on both the front and trailing edges of the injection pulse, although injection has always been from outside the stable orbit radius. This may perhaps be taken as evidence that the process is primarily a compensatory one weakening or strengthening an effect already present; an inference which is also supported by the relatively small effect of the radial

thickness between that part of the injection gun which is nearest to the equilibrium orbit, and the more remote part from which electron emission takes place. There are additional, and perhaps rather more surprising, effects in which the output is related in a critical and non-linear manner to the height of the annulus in which acceleration occurs.¹

.

Investigation of the injection process is, in the ways already outlined, greatly complicated by secondary phenomena; but there are also many known and unknown variables peculiar to each individual accelerator which must also be taken into account. These variables may conveniently be divided into two groups: primary variables, which are in the main design parameters; and secondary variables, which usually ~~usually~~ derive from and reflect constructional imperfections. The primary variables may be taken

¹ Elder, Langmuir, and Pollock Review of
Scientific Instruments 19,2 p121 1948

to include the magnetic field and vacuum chamber geometries; while the secondary variables appear in the form of magnetic and possibly electrical inhomogeneities. They may be classified as follows:

Primary Variables

Magnetic Field Geometry:

Position of the equilibrium orbit,
Variation of n with radius, and displacement above
and below the equilibrium orbit.

Vacuum Chamber Geometry:

Radial disposition of the injection gun and target,
Radial and vertical limitation of the accelerating
chamber annulus,
Gun orientation and injection pattern.

Secondary Variables

Magnetic Irregularities:

Quadrature flux components relative to azimuth,
Variation of n with radius, azimuth, and excitation,
Existence of radial flux components unrelated to the
focussing conditions.

Vacuum Chamber Irregularities:

Random electric fields due to charge accumulation
on vacuum chamber walls,

Local quadrature flux components produces by eddy currents in wall coatings, and particularly in the r.f. resonator silvering of a synchrotron.

Early experiments with the 30 MeV synchrotron quickly indicated the difficulty in recognizing and separating the many significant secondary variables; and it was also often found that the inhomogeneities which could be isolated were ~~often~~ better incompletely corrected if a large output was to be obtained; careful correction often bringing about a reduction of output rather than an increase. It was, however, rapidly appreciated that once a machine had been fairly well adjusted the most important single factor affecting its long-term performance was the quality of the available electron guns. The optimum gun position can be determined easily, and can be repeated accurately when replacing a gun; but the direction of injection relative to the gun, and the nature of the emergent beam pattern, vary considerably from one gun to another, with the result that a repeatable standard of performance is difficult to ensure.

It therefore seemed desirable to ascertain the factors influencing gun performance by, at the very least, distinguishing between emission patterns leading to high output, and others producing only low output. From this study an empirical basis for selection might be developed. It was also hoped later to control manufacture more closely, modifying the designs where necessary, and testing every gun in an auxiliary test chamber before transferring it to the accelerator for which it was aligned.

It was realized that a gun which gave a very high performance but required extreme accuracy of injection timing and emission control was generally undesirable, as this would make the betatron performance correspondingly critical. A compromise between high output and ease of control might therefore become necessary if the two requirements were found to be in any way mutually exclusive.

At the time when study of electron guns became desirable there was only one synchrotron in the Department - the 30 MeV prototype machine already referred to. A certain amount of useful information was obtained from this machine before its application

to physics problems curtailed such study. A special gun testing unit of the kind already mentioned, was therefore constructed, so that guns might be examined and tested independently of the synchrotron. A vacuum system and injection modulator were required for running the gun, and a combination of screen and probe techniques was developed for examining the beam patterns. Provision was also added, at a later stage, for ageing the guns by sustained running at their breakdown voltage; the current in the flash-over being limited by an adequate series resistance.

The work undertaken in the gun testing unit might therefore be divided into three sections: examination of gun patterns to discover their relationship with machine performance, and the most promising beam distribution; correlation of the gun patterns with electrode geometry; and ageing of the guns to withstand high working voltages.

It was hoped at a later stage to correlate this work with operational tests on the 300 MeV synchrotron which was being installed in the Department while much of the independent work on electron guns was taking place. The opportunities for such correlation have,

performance, been limited; although results have been obtained which provide a fairly coherent picture of the injection requirements. They are also consistent with, and to some degree extend, the earlier experience acquired in working the lower energy machine.

11) Early work on the 30 MeV Synchrotron

The small Glasgow synchrotron, shown in Fig 2, is nominally rated for a peak acceleration energy of 30 MeV - based on a 10,000 gauss peak field and a 10 cm orbit radius; although, in fact, the machine is only capable of about 24 MeV peak acceleration energy. This, and other performance limitations may, in general, be attributed to the rather disappointing performance of the magnet; a prototype assembly built at the English Electric Company's Nelson Research Laboratories to a design by the Accelerator Group of the Atomic Energy Research Establishment.¹

It is useful here to outline the limitations of

¹ Fry, Goward, Gallop, and Dain Nature 161 p504 1948

Fig 1 Schematic Diagram of Betatron

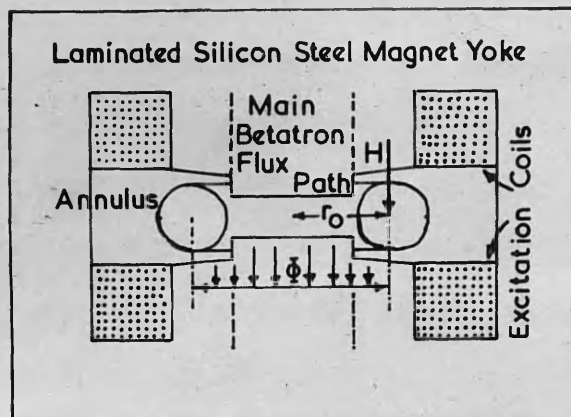
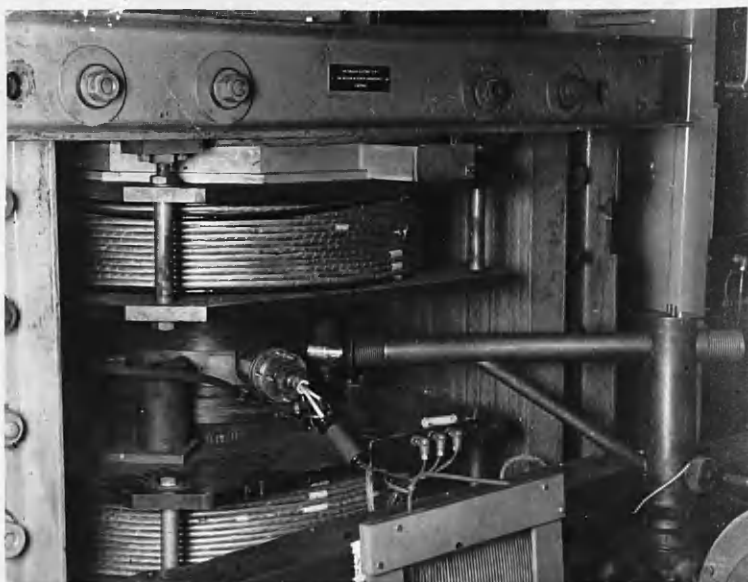


Fig 2 Glasgow 30 MeV Synchrotron

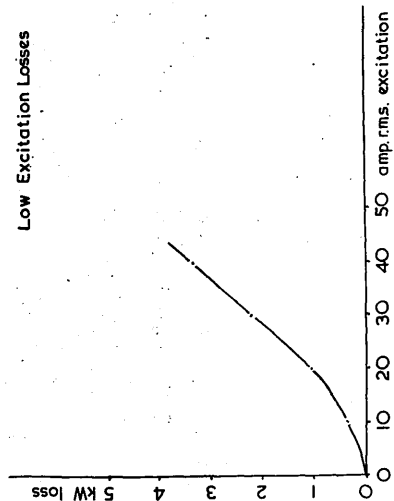
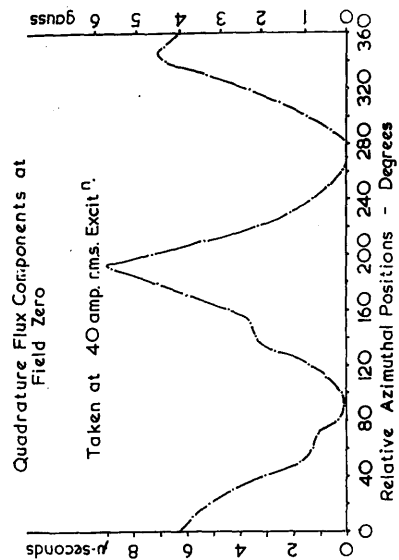
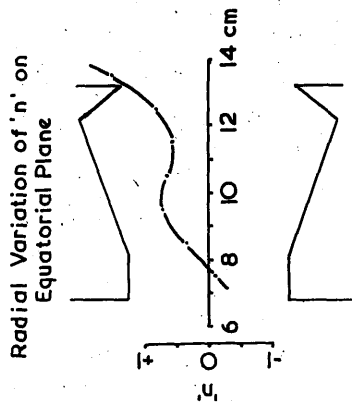
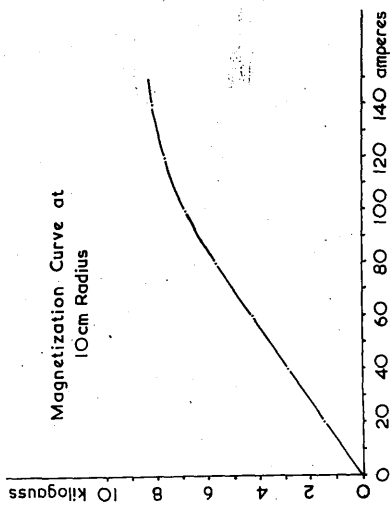


this machine before discussing the performance of injection guns placed within it; the survey will, however, be as brief as possible. Magnet characteristics are predominantly important and are fairly comprehensively represented by a magnetization curve, an equatorial plot of the radial n -value variation, an azimuthal plot of inhomogeneities at flux zero, an electrical loss curve, and a plot of the betatron orbit adjustment. All but the last of these are shown in Figs 3 - 6.

It is immediately obvious that this magnet falls considerably short of the design specification, which requires a substantially linear magnetization curve at the orbit up to 10,000 gauss. Not only does the measured curve approach saturation below 9,000 gauss: the performance of the machine noticeably deteriorates some distance below full excitation. And, moreover, the maximum energy limitation - at about 24 MeV - is accompanied by a running time limitation related to the high losses and the consequent over-heating.

The inhomogeneities due to eddy-currents and hysteresis losses, which affect the injection process, are not as seriously disturbing as the magnetization

Figs 3 - 6 Magnet Characteristics of 30 MeV Synchrotron



curve might lead one to expect: they agree closely with the characteristic to be expected from a machine of rectangular yoke construction. This machine was originally intended to operate with the initial injection at 10 kV, and the corresponding guide-field intensity 33 gauss. At 40 amperes r.m.s. excitation the overall azimuthal inhomogeneity, as shown in Fig 5, amounts to almost 6 gauss; the second harmonic component being by far the greatest, with a peak value of 2.25 gauss.

Bohm and Foldy have shown that the peak value of the forced radial oscillation, x ,

$$= \frac{h_I \cdot r_0}{I^2 + n - 1} \cdot 1$$

where r_0 is the equilibrium orbit radius, and h_I the peak flux density of the I^{th} harmonic, expressed as a fraction of the main field, itself varying radially in such a way that $H_I = H_0 \cdot r^{-n}$.

Then, in the present case, where n may be taken,

¹ D.Bohm and L.Foldy Physical Review 70 p249 1946

from Fig 4, as 0.7,

$$x = \frac{2.25 \times 10}{32 \times 2.7} = 0.25 \text{ cm.}$$

The effective radial width of the accelerating chamber is defined by the dimensions of the r.f. resonator, and is 4.0 cm. The maximum permissible free oscillation following radially displaced injection, being limited by this dimension, should clearly have an amplitude rather less than 2.0 cm. The forced oscillation will therefore, in this case, be approximately one eighth the size of the free oscillation and is unlikely to play a critical part in controlling the output from the machine. However, a similar level of output would probably be difficult to maintain at full magnet excitation, unless either the magnet inhomogeneities were partially corrected, or the injection voltage were raised to correspond with a higher and more homogeneous guide-field intensity.

The former solution was never seriously considered, because the rectangular design of yoke made a suitable correction circuit difficult to install. It would be necessary to insert thin water-cooled coils between the pole tips and the main centre yokes, and to connect them to very low value, high wattage, adjustable

resistances near by. Such an arrangement, even if only for second harmonic correction, seems undesirable if an increase of the injection voltage can yield comparable improvement. Experimental work on other similar machines indicated that a betatron output of 50 to 100 milliröntgens per minute one metre from the target was certainly adequate for a large synchrotron output. As the performance of the Glasgow 30 MeV synchrotron was improving rapidly with increase of the injection voltage, and was between 5 and 10 milliröntgens per minute at a metre from the target for 10 kV injection, it seemed sensible to concentrate on raising this voltage. Several guns operating at between 30 kV and 50 kV gave betatron outputs around 60 milliröntgens per minute at a metre, and one gun, during the period under discussion, gave 0.1 Röntgen per minute at a metre.

A serious handicap throughout this work was uncertainty about the position of the stable orbit. The orbit radius can only be measured when the vacuum chamber has been removed from between the poles, and its position may change to some extent when opening the machine equatorially to replace the vacuum chamber.

The position of the orbit is determined by an air-gap reluctance in the central flux path carrying the accelerating flux, ϕ . Alteration of this gap affects the relationship between ϕ and H , and therefore, the stable orbit radius. The graph of Fig 7 shows the extremely critical nature of the adjustment, but it must also be appreciated that the true air-gap reluctance is considerably more complicated than this graph suggests; the measured air-gap being, in fact, only one of three series air-reluctances in the betatron flux path: it is, moreover, the only one that can be measured with any degree of certainty. Fig 8 more faithfully represents the conditions involved.

The betatron flux is carried through the two betatron poles contained within a circular core inside the guide-field poles. This core is not, however, exactly circular: owing to the manner of construction it is both roughly finished and slightly elliptical; its roughness depending on the undressed surface provided by radially stacked core laminations, and its elliptical distortion resulting from the purely transverse manner in which the core is clamped. The poles themselves, although initially machined circular

Fig 7 Betatron Gap Sensitivity

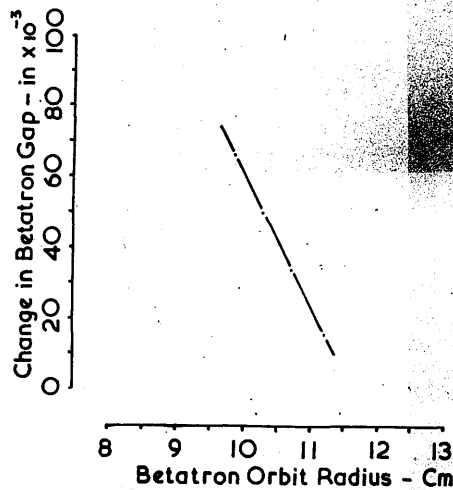
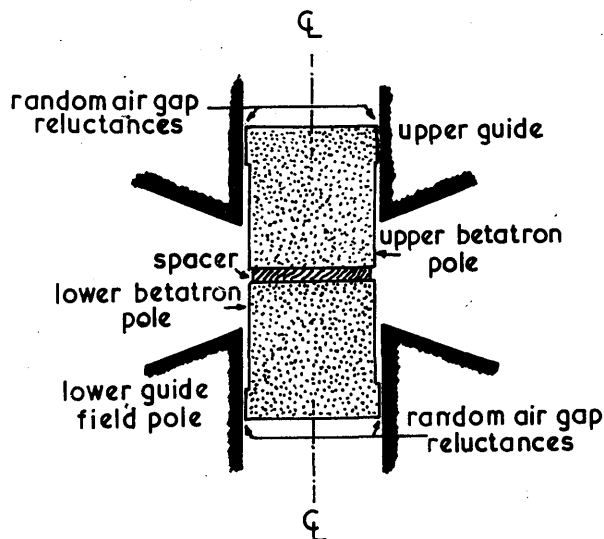


Fig 8 Betatron Gap Geometry



on the outside surfaces, are also unreliable, as serious distortion quickly results from extended operation. This may be attributed to high local iron losses in the poles themselves, and to a considerable rise in temperature in their vicinity.

To the uncertainty of the air-gap reluctance must be added a further inaccuracy in the method adopted for betatron orbit determination; for this involves estimation of a tangential point of contact on a rather flat curve. The method depends on measuring the variation of the tangential electric field with radius; the betatron orbit occurring where this field is minimum. If a number of orbital coils are placed in the equatorial plane of the magnet gap, and each contains the same length of wire but is of a different radius, then the coil which receives the smallest induced voltage indicates the position of the stable orbit. In practice relative induced voltages are plotted for different betatron gap settings, and the horizontal tangents to the various curves indicate the corresponding orbit positions. Fig 9 represents such a family of curves.

It may be mentioned that an inconsistency arose

30 MeV Synchrotron

Fig 9

Tangential Field Plot

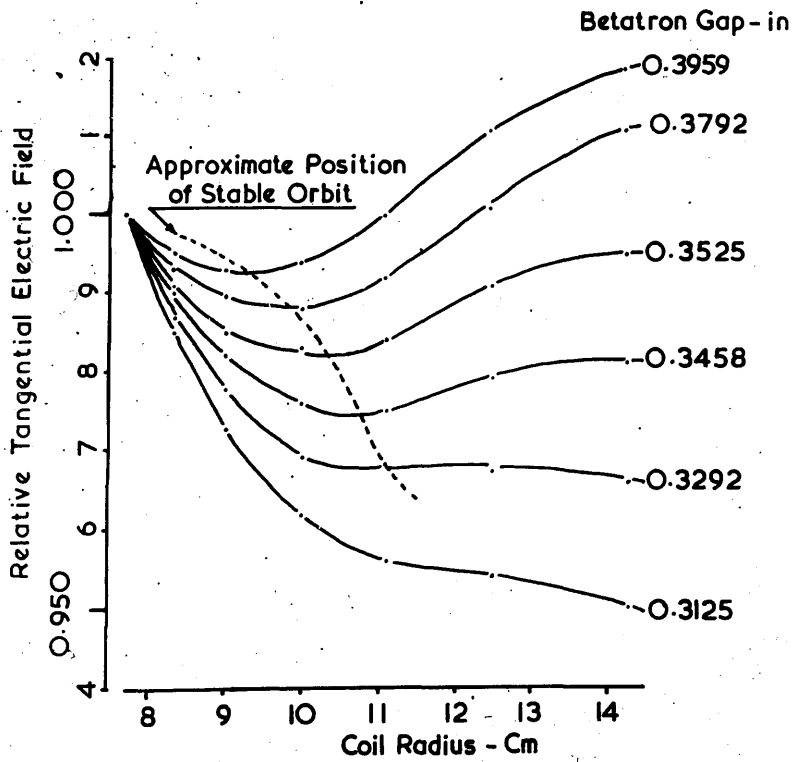
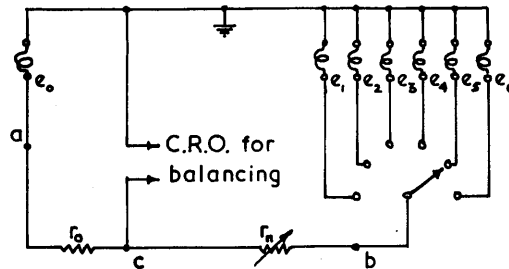


Fig 10 Circuit Diagram of Betatron

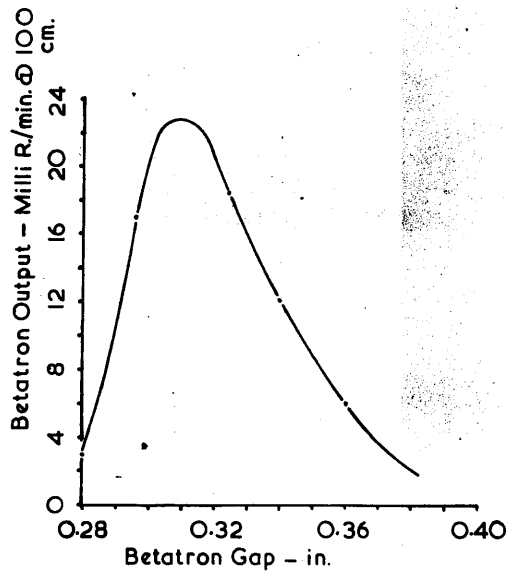


At a voltage = $-e_o$ } At c voltage = $-e_o + \frac{r_o(e_n - e_o)}{r_o + r_n}$
 b voltage = $+e_n$ }

For a null condition at c :

$$e_o = \frac{r_o(e_n - e_o)}{r_o + r_n} \quad \therefore e_n = \frac{r_n}{r_o} e_o$$

Fig 11 Output Sensitivity to Gap



the specified position of 10 cm from the centre of the machine.

The curve shown in Fig 11 has a low peak value for two main reasons: the gun was a poor one; and the disposition of the components within the accelerating chamber was unsatisfactory, as later results will confirm. The radial dispositions were as follows:

Gun filament radius	12.0 cm
Target radius	8.5 cm
Inner and outer limits of r.f. resonator	8.1 cm 12.1 cm.

It was later found that 0.2 cm margin was essential between the radial positions of the gun filament and outer resonator wall if the output was not to be impaired.

iii) Betatron Characteristics of the 30 MeV Synchrotron

It is convenient to classify the curves relating betatron output to magnet excitation, injection voltage, and filament emission as the Betatron Characteristics of a machine, because a glance at them will rapidly establish the relative importances of the most critical variables associated with a machine. An early set of betatron characteristics for the 30 MeV synchrotron is shown in Fig 12. The

shapes of the curves may be explained as follows:

Excitation Characteristic

The initial rise with excitation may be attributed to the increasing gain of energy per orbital turn, caused by the proportional increase in $\dot{\phi}$, and the corresponding reduction of the total orbit length and probability of collision with gas molecules. That the output begins to deteriorate near full excitation may be explained by the increasing importance of quadrature flux components at injection.

Injection Energy Characteristic

That the output will increase as the injection energy is increased may be expected for two main reasons: the higher injection energy will bring the condition at injection further out of the inhomogeneous magnetization near to flux zero; and it will also reduce the related adverse effects of beam current induction and space charge during the injection period.

Injection Current Characteristics

It should be noted that this particular characteristic is not representative: the output peaks at an appreciably higher injection current normally (around 200 - 300 ma.) and is not evident at all until a current

of perhaps 50 ma. has been produced. The failure to obtain any output for emission less than a critical value may be taken as direct evidence that some induction effect such as already outlined by Kerst does in fact take place.¹ Moreover, the initial zero component of the Current Characteristic can be eliminated altogether by using an orbital pulsed coil at the moment of injection.² The slow deterioration in output for emission increase above the optimum value may be accounted for by space-charge limitation within the annulus.

It should be noted that the two characteristics which pass through peak values (the Energy Characteristic also turns over in the same manner at about 50 kV) have markedly smaller slopes above the optimum than below it. From an operational point of view it is therefore generally desirable to run at conditions involving passing through the optimum; adjustment then being very much less critical.

¹ D.W.Kerst Physical Review 74 p503 1948

²² J.D.Lawson A.E.R.E. Memo E1/M2 1949

These characteristics clearly define the best betatron operating conditions; but because the synchrotron output is also directly dependent on the betatron performance, and the betatron-to-synchrotron transfer efficiency is high, they also predominate over all other factors affecting the synchrotron output.

iv) Early Electron Gun Experiments on the 30 MeV Synchrotron

Injection into the 30 MeV synchrotron is effected by means of a Kerst type electron gun with the geometry shown in Fig 15. The anode is at earth, or possibly vacuum chamber, potential, while the filament and shield are together pulsed negatively whenever an emission pulse is required. The filament is a uniformly wound tungsten helix which, in the first guns, was a bright emitter, but is now generally thoriated to obtain higher emission and longer life. The following account of experimental work on the 30 MeV machine relates only to the period when bright emitters were used, but there is no significant difference between the emission patterns of bright and thoriated filaments, although the latter exhibit occasional transient idiosyncrasies which are clearly

Fig 14 Data Characteristics

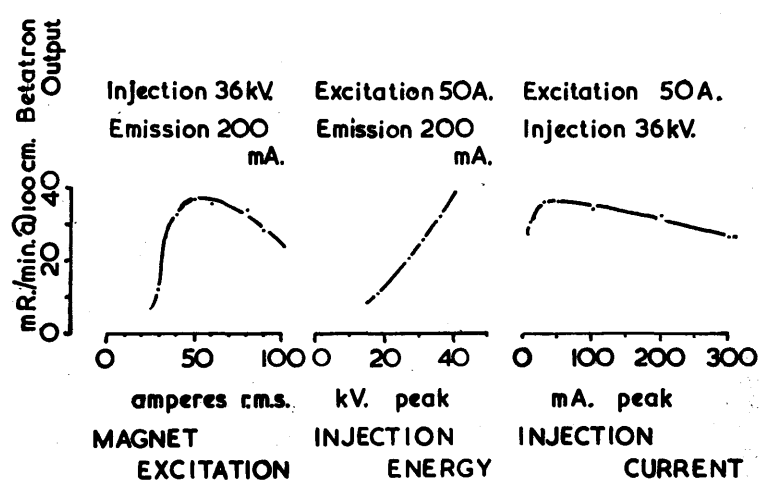
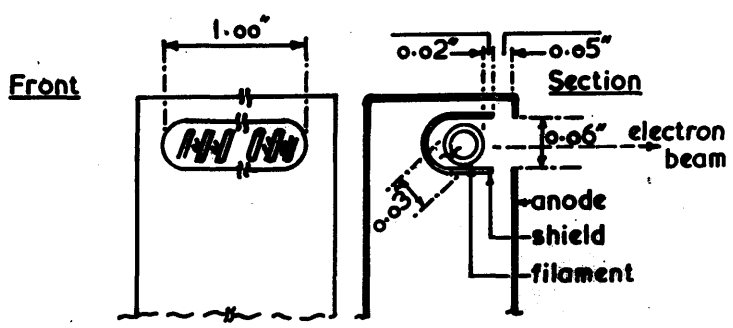


Fig 15 Out. Dimensions



Not to Scale: The Dimensions are to be taken as an Approximate Indication only.

the result of changeing distribution of filament surface thorium.

The elementary behaviour of the guns is simple enough: the mouth of the shield and the anode aperture provide an accelerating, and to some extent focussing field, through which electrons are accelerated from the filament into the vacuum chamber annulus. The back of the shield serves primarily to restrict useless diode current to the rest of the anode (which shields the orbital electrons from the field produced by the negatively pulsed cathode) and may also help to conserve heat in the filament vicinity.

At the time when these experiments were carried out very little was known about the electron-optical characteristics of these guns, but it was assumed that the emission pattern would bear some direct relationship to the gun geometry; that it might, roughly, appear as an ellipse with the major axis lying along the length of the anode aperture and the minor axis lying across it. It was also expected that the beam would widen if the filament were moved closer to the mouth of the shield, and that the increased field gradient near the filament would

increase the emission per watt of filament power.

The first tests carried out with the early guns involved rotation of the gun about a vertical axis, so that the tangential angle of injection might be altered. Readings of the betatron output were recorded as a function of tilting for eleven different radial positions of the gun. The results are plotted in a series of curves shown in Fig 14. The conditions of test were as follows:

Magnet Excitation	50 amperes r.m.s.
Betatron Gap	0.316 in.
Vacuum Pressure	10^{-5} mm. Hg.
Injection Voltage	27 kV.
Emission	Set to Optimum.
Target Radius	9.0 cm radius.
Resonator Inner Limit	8.3 cm radius.
Resonator Outer Limit	12.3 cm radius.

It is clear from these curves, and particularly from the ones where the gun is near to the equilibrium orbit, that the output increases as the radius from which injection takes place also increases. The individual curves vary considerably in outline, but their peak values, when plotted against the radius of injection, indicate a surprisingly smooth relationship, as demonstrated by Fig 15. It will be noted that the derived curve has a peak value when the injection radius

Fig 14 First Gun Filt Tests

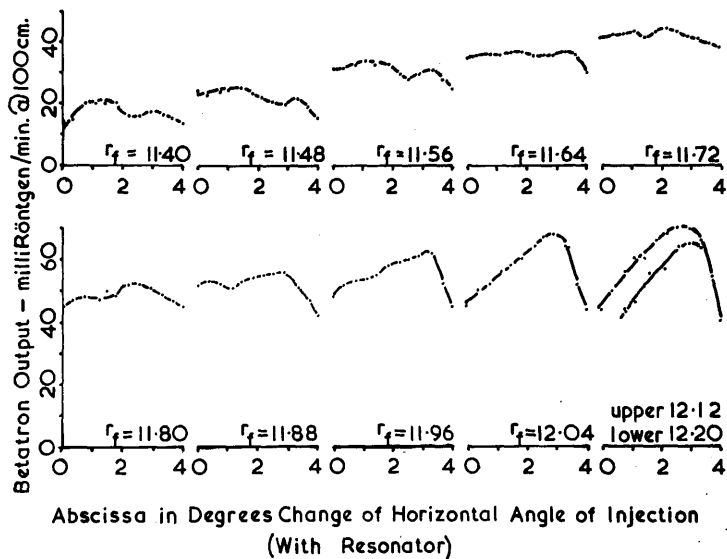
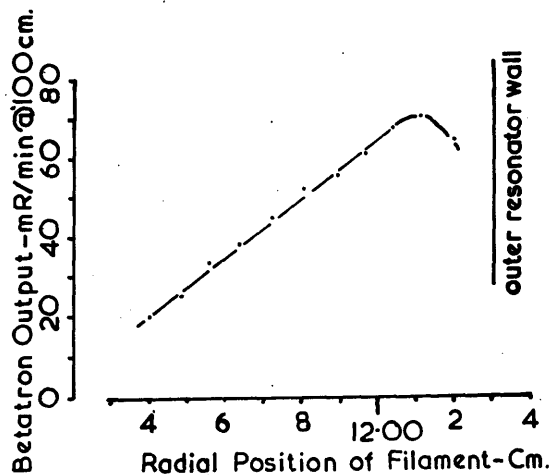


Fig 15 Derived Results



is 12.1 cm; the radial optimum in this instance being determined less by the magnet geometry than by that of the vacuum chamber; for the maximum output occurs only 0.2 cm from the resonator wall, and all other tests have shown this to be the critical separation after which interference between the resonator and the injected beam becomes appreciable.

This interesting correlation is secondary to the main purpose of the test, which was to determine the sensitivity of the machine to angular displacements of the gun. It will be seen that when the gun is at the optimum radial setting the injection angle about a vertical axis is critical to approximately $\pm 2\frac{1}{2}^\circ$ for a loss of half the output. A slightly less critical condition applied for the twisting of the gun about a radial axis; Fig 16 suggesting the corresponding angle to be $\pm 4\frac{1}{2}^\circ$. It was felt that, for ease of setting, both angular sensitivities were very much too high and should, if practicable, be reduced.

The curves for various radial settings shown in Fig 14 were unnecessarily complicated by the presence of the resonator; a second series was therefore taken without the resonator in position, and generally

covering a rather larger series of injection radii. The results are shown in Fig 17, which also includes two transferred characteristics from Fig 14, for comparative purposes. A derivative curve of the peak output plotted against the radius of injection is reproduced in Fig 18, together with a radial plot of the equatorial n -value, based on the curve in Fig 4. It has been argued that injection will be most effective from the edge of the stable annulus, where $n = 1$, and Fig 18 would appear to support this contention.

There is a factor of 2.4 between the maximum outputs obtained with and without the resonator in position. It was therefore decided to move the resonator radially outward to the best position indicated by previous measurements. At the same time, unfortunately, it was necessary to replace the electron gun, so complete experimental continuity could not be maintained. However, with the new gun, and all other variables except the vacuum chamber geometry unaltered, a companion series of curves to those of Fig 14 was plotted. The vacuum chamber geometry was as follows:

Fig 16

Gun Twist Test

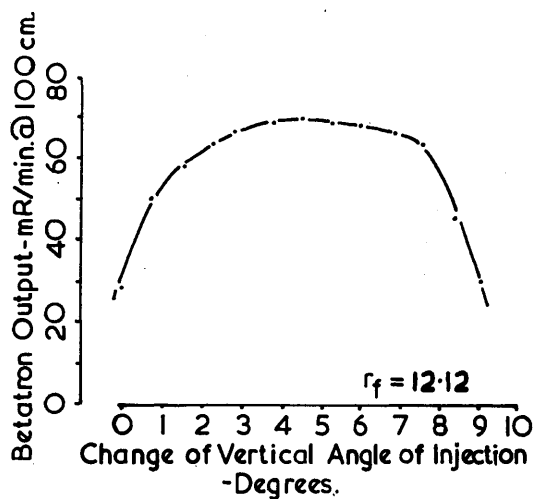
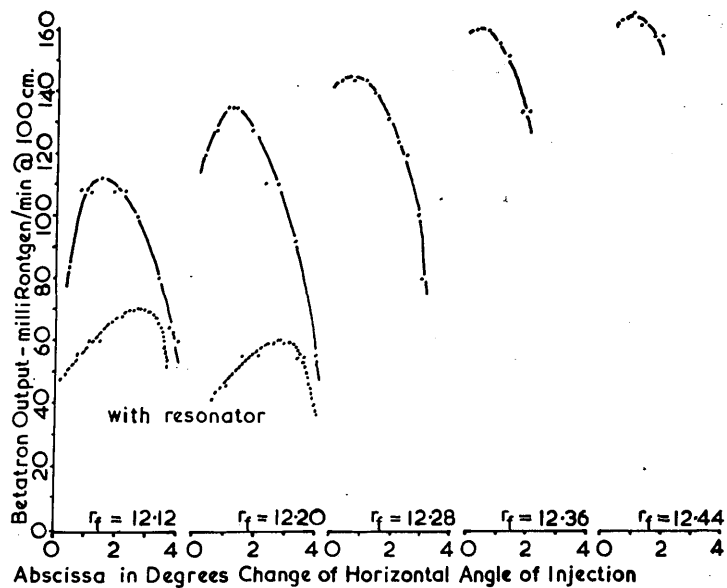


Fig 17

Second Gun Tilt Tests



Target	9.3 cm radius.
Resonator Inner Limit	8.8 cm radius.
Resonator Outer Limit	12.9 cm radius.

The results obtained with the second gun are shown in Fig 19: they are noticeably smoother and generically more similar than the first series of curves, but are also less sharply peaked than the second. The angular sensitivity is not appreciably altered.

v) Implications of 30 MeV Synchrotron and Gun Tests

The work already described was all carried out during the commissioning period of the 30 MeV synchrotron. When the machine was clearly giving as large an output as might be expected without resorting to inordinately complicated correction techniques it was turned over to nuclear physics applications. Further opportunities for study of the performance were then drastically curtailed.

It had already become obvious that the information contained in measurements of the twist and tilt type could only be properly examined if the distribution of the injected electrons was better known. The implications of the available results were certainly surprising -

Fig 18 Output and 'n' at injection

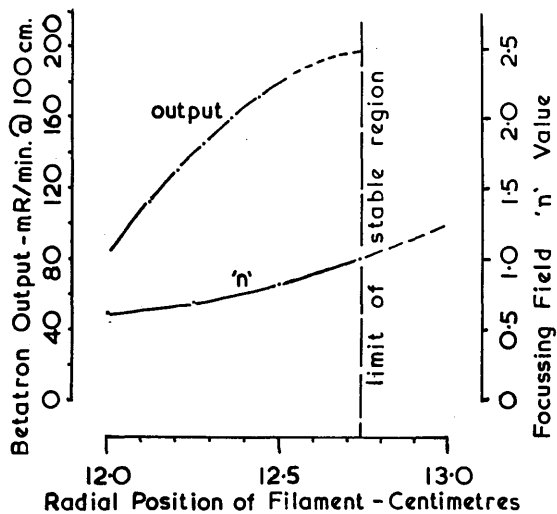
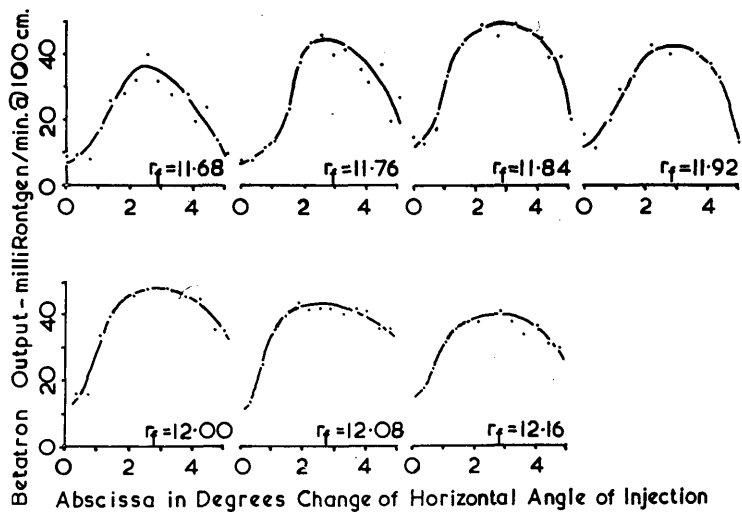


Fig 19 Third Gun Tilt Tests



that distribution angles of $\pm 2\frac{1}{2}^\circ$ and $\pm 4\frac{1}{2}^\circ$ might be involved - for the geometry of the guns did not seem likely to provide a concentrated injection pattern. If the pattern were not concentrated the injection process might well depend on a critical balance between the number of electron injected with an inward radial velocity, and the number with an outward velocity. Arguments about the large initial circulating current and its effect on the stable orbit suggest that such considerations may indeed be important. It was, however, subsequently found that the injection pattern was usually concentrated within angles closely corresponding to those quoted.

The initial argument for building some type of gun testing unit was therefore based directly on the early twist and tilt curves, which were clearly of much greater potential than actual value. Some of the other considerations, such as the ability to set up and test guns outside the machines on which they were to be used, have already been mentioned: what is perhaps of primary importance is that the external tests are clearly complementary to performance tests on the machines. This complementarity, at first only recognized in general terms, has become increasingly evident as independent gun testing has continued; it has provided the central motivation of the following work.

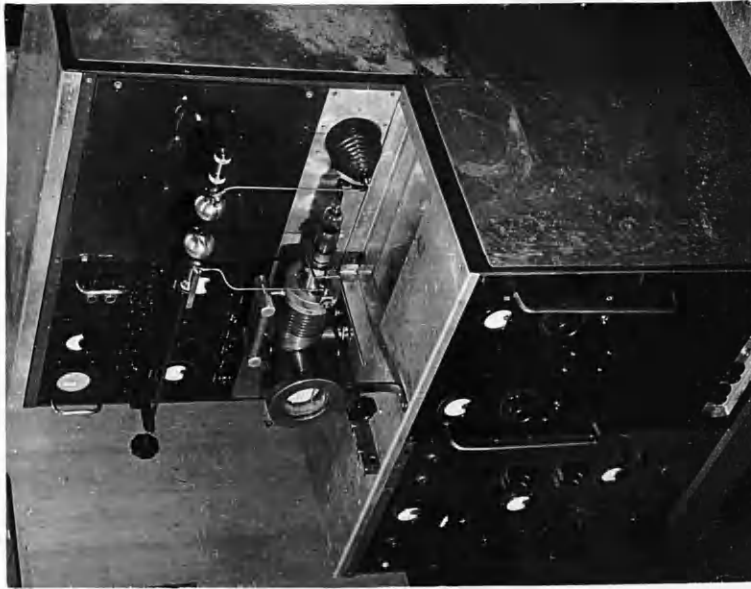
A GUN TESTING UNIT

1) Basic Structure

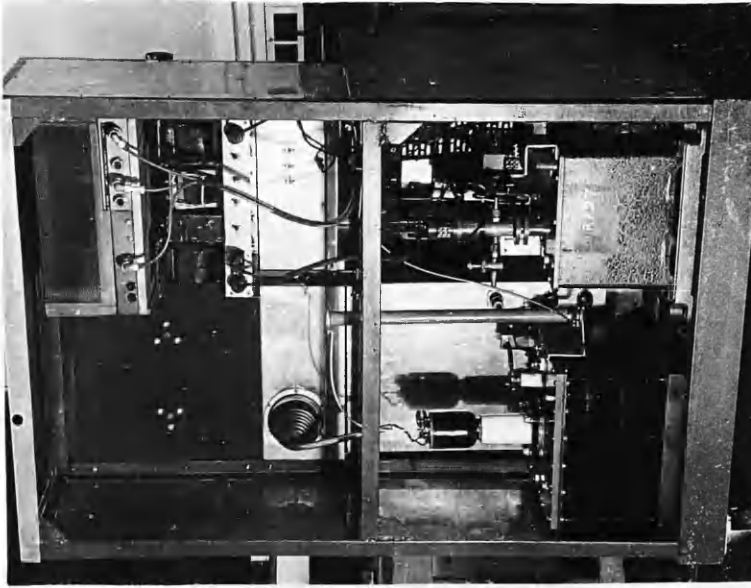
It was decided at the outset to build an entirely self-contained installation for gun testing. This apparatus was to be assembled on a welded steel framework 39in x 36in in plan area, supported on four ball bearing castors. The main base was to be fabricated from 2in x 3in rolled steel channel, with various additional supports constructed from $1\frac{1}{2}$ in x $1\frac{1}{2}$ in angle iron. The main superstructure, also of $1\frac{1}{2}$ in angle iron, would rise 30in at the front, to provide a 19in deep test platform; behind this a further section would rise another 24in to allow mounting space for equipment built onto standard 19in panels. Similar panels would be carried in front of, and below the main test platform, but the greater part of the lower volume of the equipment would be occupied with vacuum pumps, pulse transformer, and the injection modulator.

The completed unit is shown in Fig 20; and Fig 21 shows, in block schematic form, the distribution

Fig 20 The Complete Gun Testing Unit



Front



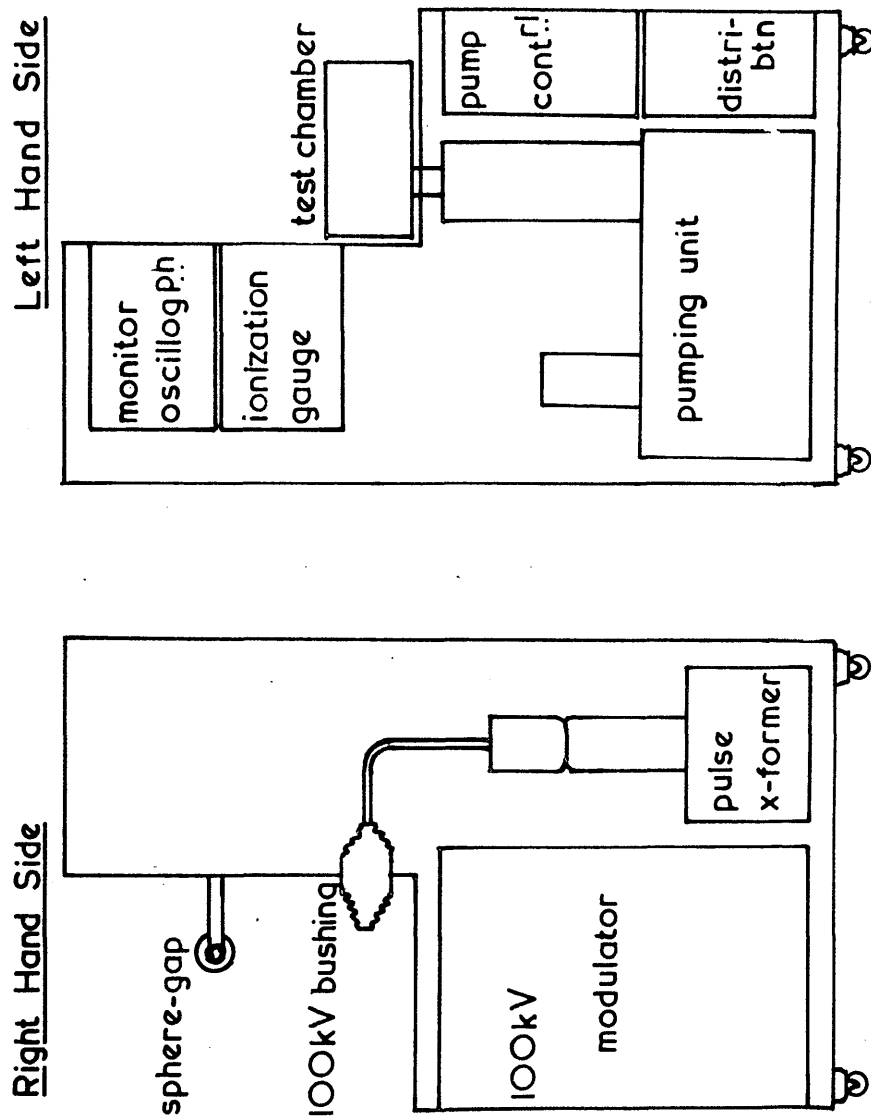
Rear

of the main components. Of these the most important are the vacuum chamber and pumping equipment, the pulse modulator and gun filament supply, and the monitor oscilloscope.

11) The Vacuum System

It is necessary to test the injection guns in a vacuum rather better than 10^{-5} mm. Hg.; and because there is likely to be considerable outgassing from the gun surfaces during ageing, and possibly as the result of occasional flash-overs, it is practically desirable that the measured vacuum pressure should be less than 10^{-6} mm. Hg. To meet this requirement the gun testing chamber is pumped by a 3in oil diffusion pump situated immediately underneath it. An oil trap separates the pump from the chamber, and the chamber is electrically insulated from the rest of the system by a 4in Perspex flange; the latter provision being necessary if the total electron emission to the chamber is to be measured. Two test chambers have been built, the first of which is shown in Fig 22. The main cylinder will be seen to carry four variously shaped side entries, the lowest of which, with the Perspex flange attached, couples onto the oil trap

Fig 21 Layout of Gun Testing Unit



above the pump and supports the whole chamber assembly. The port on the right of the photograph carries the electron gun to be tested, and another Perspex flange fitted here enables the gun anode to be insulated from the body of the chamber. In this case the flange diameter, $2\frac{1}{4}$ in, corresponds with the size of port on the 30 MeV synchrotron chamber. The port on the left of the chamber is an ionization gauge mounting, and that on top a recessed observation window. (Guns for the 30 MeV machine may be inspected from the filament ends but the 100 kV guns for the 300 MeV machine have side shields which make this impossible.) The front of the chamber carries a 6in diameter threaded flange onto which a $6\frac{1}{2}$ in clamping ring may be screwed. This either holds a 7.5mm plate glass window or the flange of a probe unit to be described in a later section.

The second chamber is for testing 100 kV electron guns for the 300 MeV synchrotron. It differs from the first chamber primarily in the size of the gun port, which is $4\frac{1}{4}$ in in diameter to correspond with the port dimensions on the synchrotron itself. The second chamber is shown in Fig 23, and will be seen in other respects to differ little from the first one. The chamber is mounted

Test Chambers

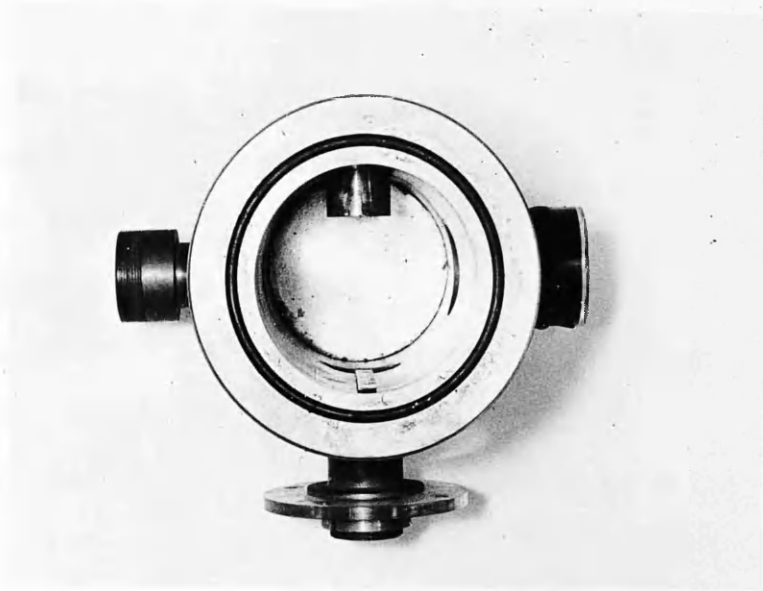


Fig 22 Test Chamber for 30 MeV Synchrotron Guns

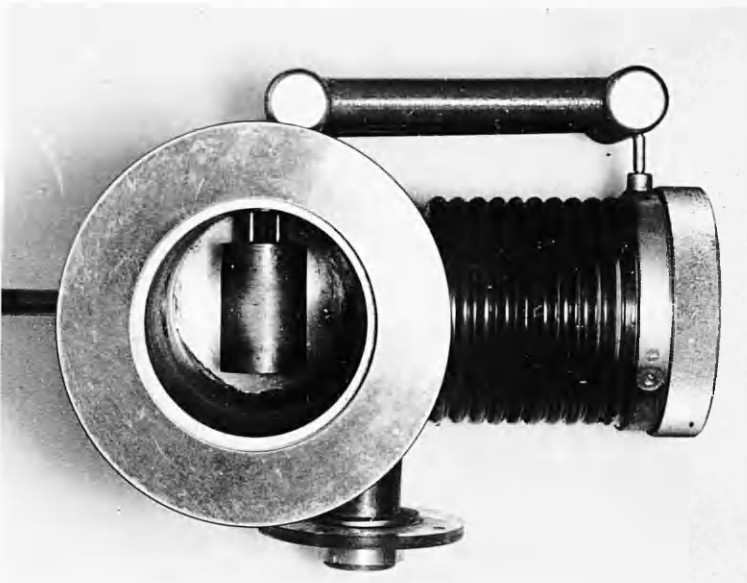


Fig 23 Test Chamber for 300 MeV Synchrotron Guns

slightly eccentrically on the pumping port, to allow for the increased length of the gun and its mounting. An inspection window is not fitted, as there is no direct view into the sides of the gun; but a liquid air trap, which greatly increases the vacuum stability, has been added immediately behind the position of the gun in the chamber.

The gun port is both longer and mechanically different from the low voltage gun mounting, for the insulation between the gun mounting and the body of the test chamber has been increased to withstand 100 kV injection pulses. This makes it possible to insert a series resistance of 30,000 ohms between the gun anode and earth; the arc current during flash-over being limited by this means to about 3.3 amperes peak. The current has, of course, a very low mean value, and the resistance assembly, which may be seen above the gun port, is a multiple carbon unit with a continuous rating of about 20 watts.

The high voltage insulator on the gun port is an annular Araldite casting, machined on the outside and cold resin mounted onto a tubular brass port-root which is an integral part of the test chamber.

Casting of large Araldite sections - particularly of a 100 kV bushing leading the pulse voltage out to the main testing platform - proved a little tricky, in that very long stoving times at relatively low temperatures are necessary to avoid excessive internal stressing of the material. If care is taken, however, a large mass of almost any shape can be fairly easily cast. The surface characteristics of the material are not particularly satisfactory and may lead to quite considerable leakage currents, so in all cases surface corrugations have been added to reduce the losses. (It is during the turning of these corrugations that internal stresses may become dramatically - and disastrously - evident.)

The pumping unit is simple and conventional, and comprises the 3in oil diffusion pump, a Speedivac rotary backing pump, and a control unit. The control unit includes the usual circuitry for vacuum pressure, water-flow, and no-volt protection; but this protection is to some extent simplified by cascading the supply connections as far as possible; the oil pump being operated through the backing pump supply, the ionization gauge through the oil pump supply, and the gun modulator

through the ionization gauge supply. Various additional protective controls are inserted at appropriate points along the chain.

111) Gun Supplies

The electron guns operate with a 50 c/s a.c. voltage on the filament, usually at about 6 volts r.m.s.; and both filament and shield are pulsed negatively for a few microseconds between five and fifty times a second. The 30 MeV machine operates at mains frequency and therefore has a pulse repetition frequency of 50 c/s: the larger machine, on the other hand, operates at 5 c/s and requires a correspondingly lower repetition frequency. In the testing unit provision is therefore made for injection pulses at any voltage up to about 120 kV, with repetition frequencies of 5 c/s, 10 c/s, 25 c/s, or 50 c/s.

In both synchrotrons the injection pulse is approximately rectangular, being supplied from a delay-line type of modulator giving a pulse length of about 5 microseconds. The first gun testing modulator was also of the delay-line type, although rectangular pulses are not really necessary for testing purposes, and have yet to be shown important to the injection

process. Delay-line modulators are themselves to some extent undesirable, as the voltage of the generated pulse is only half of that to which the line is charged; a condition leading to poor utilization of the high voltage equipment, and to a rather bulky and costly installation.

By sacrificing the pulse shape and using a condenser in place of the delay-line a steep-fronted exponential pulse of height closely approximating to the charging voltage may be obtained. A mercury thyratron rated for 10 kV peak forward anode voltage - the B.T.H. BT 45 for example - may therefore be used to produce a pulse of about 80 kV peak value on the resistive load of a 1:9 pulse transformer. This arrangement was, in fact, the basis of the first high voltage modulator; the pulse transformer being a special 100 kV unit designed particularly for application to synchrotron injection circuits by the Research Department of Metropolitan Vickers Ltd., Trafford Park, Manchester. In the modulator circuit adopted the pulse-forming capacity was 0.02 mfd, and the transformer secondary load 50,000 ohms; the nominal time constant being 10 microseconds. No appreciable

self-oscillation was discernable on the output pulse-shape although the normal load for the transformer is only 5000 ohms.

An 80 kV peaked pulse is quite acceptable for injection pattern testing but is totally inadequate for ageing 100 kV guns. The voltage to which the guns are aged should exceed the final running voltage by a fairly safe margin, and the fact that the tested gun is subjected to considerable mechanical vibration in the synchrotron which it does not undergo during testing makes this margin doubly necessary. Moreover, the time taken to initiate breakdown may be longer than the period during which the pulse voltage exceeds the breakdown value, and flash-over may not occur. If the pulse length on the test unit is appreciably shorter than the pulse length encountered on the synchrotron itself gun ageing may prove entirely unsatisfactory. For all these reasons it was decided to build a considerably larger modulator for 100 kV gun ageing. It was also thought desirable to calibrate the pulse voltage against a sphere-gap as well as against the usual oscillographic display, as the sphere-gap might reveal some of the inconsistencies of ionization and

breakdown that also occur in the gun - the differences in gas pressure in the two cases having, of course, to be taken into account.

The larger modulator imposed, above all else, a particularly formidable space problem; for it was desirable that the integrity of the test unit should not be impaired by this necessarily larger addition. It was, in fact, important that the completed modulator and power supplies should fit within a volume 18in x 20in x 30 in; a task only made possible by widespread use of high voltage metal rectifiers. The completed modulator is shown in Fig 24; and the two main components, with the back of the power stack removed, in Fig 25. The square chassis, which bolts onto the lower face of the power stack, contains all the auxiliary power supplies and the complete electronic assembly; the 15 kV voltage multiplier c.h.t. supply, and the 0.02 mfd pulse-forming condenser are, however, carried on the upper assembly.

A complete circuit diagram of the modulator is contained in Fig 26. The first valve, a 6SN7 twin triode, operates as a multivibrator with switchable frequency control, normally set at 5 c/s, 10 c/s,

100 kV Modulator

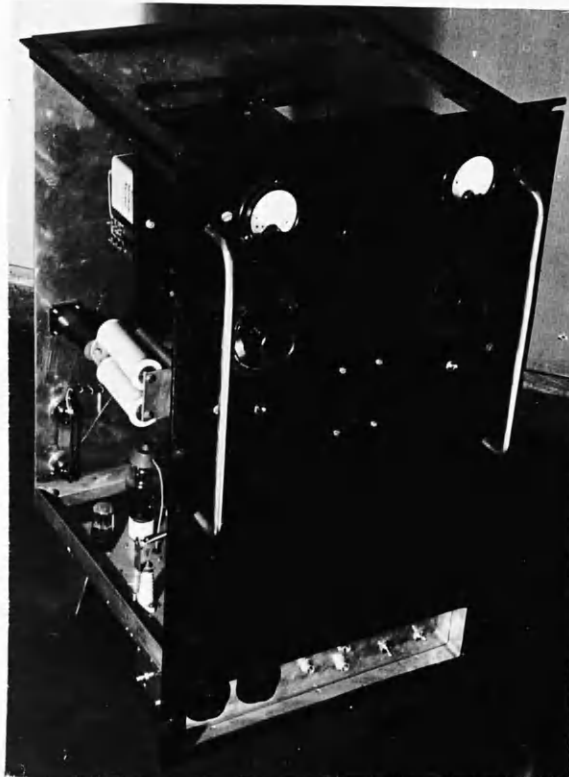


Fig 24 The Complete Modulator

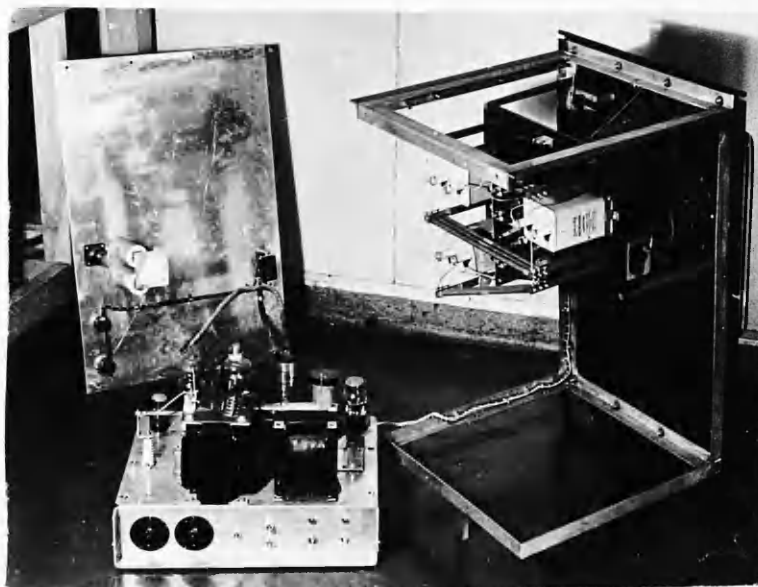


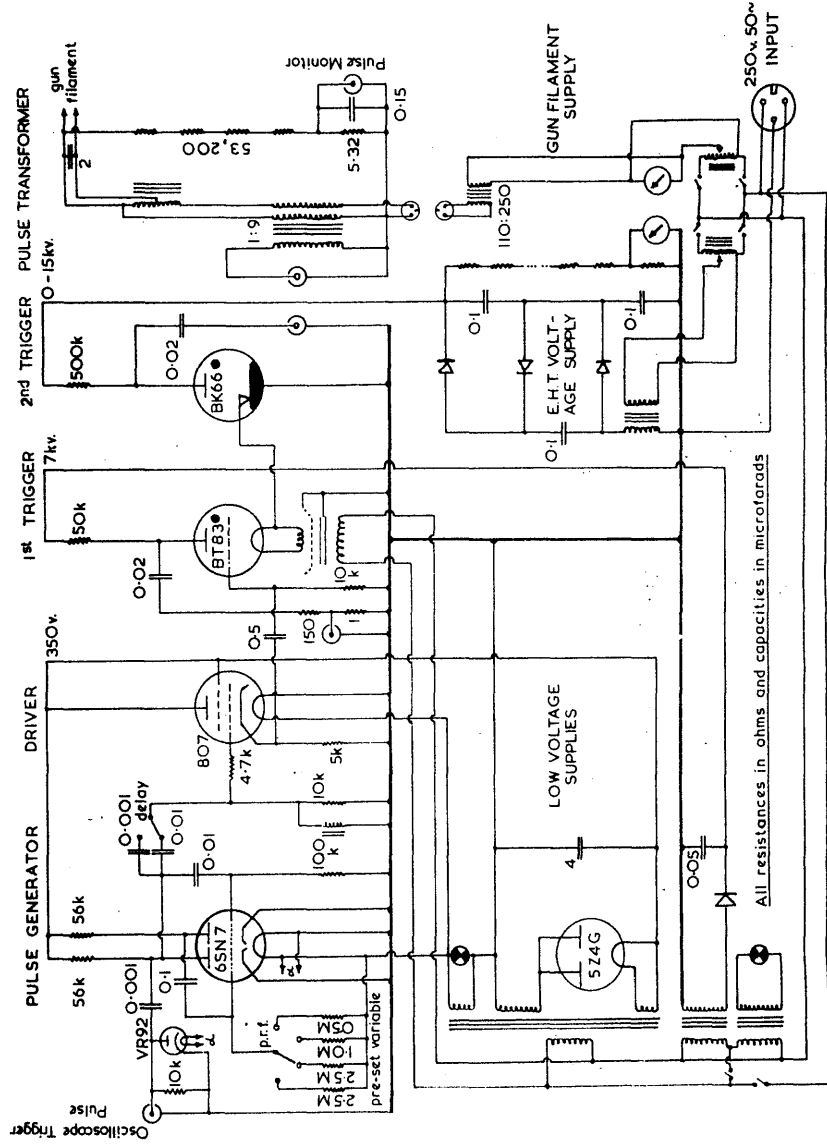
Fig 25 The Main Assemblies

25 c/s, and 50 c/s and held at sub-multiple mains frequency by a 50 c/s mains frequency tapping from the valve heater supply. This valve operates an 807 beam tetrode capable of triggering a B.T.H. type BT 83 hydrogen thyatron. The 807 is coupled through a simple L-C delaying circuit which holds the modulator pulse back until an undelayed trigger pulse has set the monitor oscilloscope sweep in action. The BT 83 discharges an 0.02 mfd condenser charged to 7 kV into the igniter of a B.T.H. BK 63 ignitron. This ignitron is the main pulse trigger and discharges another 0.02 mfd condenser which can be charged to any voltage up to 15 kV. The discharge takes place through the 1:9 pulse transformer and the 50,000 ohm load resistance. It was estimated that, if the rise time of the front edge of the pulse were 0.25 microsecond, the output voltage would be less than the theoretical value by only about 2.5 percent. With a 15 kV charging voltage the peak pulse output voltage might therefore be about,

$$15 \times 10^3 \times 9 \times 0.975 = 130 \text{ kV.}$$

The pulse height was certainly of about this value, but exact calibration of the output was difficult

Fig. 16
Circuit Diagram of 100 KV Isolator



and the problem will be discussed in a later section.

Filament supply for the gun under test is a little complicated by the fact that the filament must carry the full pulse voltage. This involves not only high voltage insulation but also a low value of capacity in the filament supply system. Fortunately for this application the pulse transformer is supplied with a bifilar secondary winding, so that the filament power may be taken to a small auto transformer at the top of the pulse transformer high voltage bushing. The bifilar winding is supplied from a 110 volt isolating transformer which is in turn supplied from the a.c. mains through a Variac transformer. No provision has yet been made for monitoring the filament power, as this has not proved an important factor in gun performance. The filament supply system closely corresponds with the provision on both Glasgow synchrotrons, so that, provided the power rating of the test unit supply is always well above that actually required, there will be no excitation problem on the accelerators themselves. This has invariably been the case. Filament rating has always been based on the peak emission current, and this alone has been monitored.

iv) Monitoring Facilities

In order to measure the injected current the total flow to the chamber walls must be determined. This can easily be arranged by inserting a small resistor between the test chamber and earth, but it is important that the gun anode should not also be at chamber potential. For the filament-and-shield to anode capacity is relatively high, and large, spiky pulses appear on the monitoring resistance, through differentiation of the injection voltage pulse through this capacity; this can, however, be avoided by earthing the anode separately and directly. It was in order to provide these electrical separations that the two Perspex flanges were fitted to the pumping and gun ports of the test chambers. Even with the anode earthed, and more or less complete electrostatic shielding thus effected, some voltage break-through and differentiation still takes place; it is therefore usual to add a small amount of shunt capacity across the monitor resistance to suppress the spurious transients.

During the period in which a delay-line modulator was being used a pulse-peak vacuum-tube voltmeter was also used; a relatively simple device with a low impedance charging circuit and a long discharge time-constant,

shown schematically in Fig 27. However, as exponential pulses and lower pulse repetition frequencies were adopted the disadvantages of this type of metering soon became apparent - particularly when a certain amount of integration was being added to eliminate differentiation spikes. It then became convenient to fit to the monitor oscilloscope, which had previously been used only to ensure that pulse shapes were satisfactory, a calibrated ordinate shift, so that pulse heights could be measured accurately at any frequency and for any pulse shape - the exact interpretation of a complex pulse shape being under the control of the observer. This method proved so successful that no further attempts at electronic metering have since been considered.

As already mentioned, the oscilloscope is triggered by an undelayed pulse from the multivibrator in the gun modulator. The oscilloscope itself is a commercially built monitor unit to which the metered shift control has been added in the Department.¹ The

¹ To A.E.R.E. Type 1000 specification.

instrument is commonly used for monitoring the total gun emission, or, when a probe is being used, the probe current. It may also be used for pulse voltage calibration, using a combined resistance-capacity voltage divider and modulator load on the pulse transformer secondary. Provision is also made for coupling the oscillograph into various places in the modulator circuitry, but such inspection has so far proved unnecessary: for checking the various multivibrator frequencies it is not particularly suitable, and a general purpose laboratory instrument has proved more convenient.

When the early modulator was removed, a separate timing unit for driving it, and the pulse-height valve-voltmeter already describe, were removed as well. After re-arranging the remaining auxiliary equipment space was made available immediately above ^{the} bushing carrying the 100 kV pulse to the test platform for a standard 62.5 mm sphere-gap, to be used in pulse voltage calibration. This gap, and the work carried out with it will be discussed in the following section.

TEST TECHNIQUES

1) Fluorescent Screens

The simplest and quickest way of testing small electron guns is normally to direct the electron beam onto a fluorescent screen, and to observe the visible pattern that results. This is not, however, such an easy method for examining the behaviour of injection guns for synchrotrons; for here it turns out both difficult to use and crude in its result. It is difficult to use because of the destructive effect of the high energy and large current electron beam, and because of the rapid accumulation of electric charge on or within the fluorescent material. The crudeness, which is perhaps only the result of insufficient study of fluorescent materials and their characteristics, arises from early saturation of all the phosphors used.

There is little point in describing at length the first attempts at making satisfactory screens;

they were, in general, coated on glass and then aluminium-backed by an evaporation process. Aluminium was first added as an opaque covering to suppress the very powerful light cast onto the screen from the early bright emitting filaments. Later the aluminium became more important as a means for removing electric charge from the screen surface. A more successful manufacturing technique has involved using 0.0002 in aluminium foil as the foundation for the screen. This is clamped between $3\frac{1}{2}$ in concentric rings and is then painted on the surface which will face the observer rather than the gun with the fluorescent material being used.

The method depends for its success on extremely careful preparation of the foil surface before the coating is applied; this involving preliminary cleaning with an effective grease solvent and subsequent etching with fine carborundum powder lubricated in a moderately strong solution of caustic soda. Neither the caustic soda alone, nor the carborundum powder lubricated with water provides a satisfactory surface; the inevitable result being that coating and foil quickly come apart. This has sometimes happened surprisingly violently;

large slabs of the coating being hurled intact against the front window of the test chamber. The effect does not appear to result from drying out of the phosphor and its base; although this does occur, but slowly and without any appreciable outgassing during bombardment: it seems rather to depend on the accumulation of charge within the screen material; an effect which would clearly worsen as foil and coating began to come apart, and which might easily lead to the violent final fractures observed.

The binding material used to hold the fluorescent powder together and onto the foil is also rather critical, and it cannot really be argued that complete success in screen binding has yet been achieved. From a purely mechanical standpoint Perspex cement, or indeed a simple solution of Perspex in chloroform, is quite without parallel, but the electrical properties it exhibits make it quite unacceptable. It is liable to accumulate large amounts of local charge which take unusually long to leak away toward either the foil or the periphery. The resultant long persisting distortion of the electron pattern was originally and falsely attributed to the erratic

behaviour of thoriated filaments, which have since proved a great deal more stable than at first seemed to be the case. A second difficulty with Perspex used as a binder is that it quickly blackens at the points of high intensity bombardment. The blackening appears on the coating surface nearest to the foil and does not penetrate deeply into the screen material. It nevertheless greatly attenuates the brightness of the fluorescent pattern observed at the front. An example of the effect is shown in Fig 28, which is a photograph of the screen pattern after approximately ten minutes bombardment with 80 kV electrons in a peak pulse current of 250 ma. with a repetition frequency of 50 pulses per second.

A binding material which is very much more satisfactory electrically is sodium silicate. It is used as a solution in water and is air dried. It does not accumulate charge, nor does it blacken rapidly, as the extended test represented in Fig 29 clearly demonstrates. It is nevertheless difficult to use in such a way that good mechanical properties are obtained. Although, like Perspex, it does not outgas seriously when subjected to electron bombardment,

Fig 27 Pulse-height Valve Voltmeter

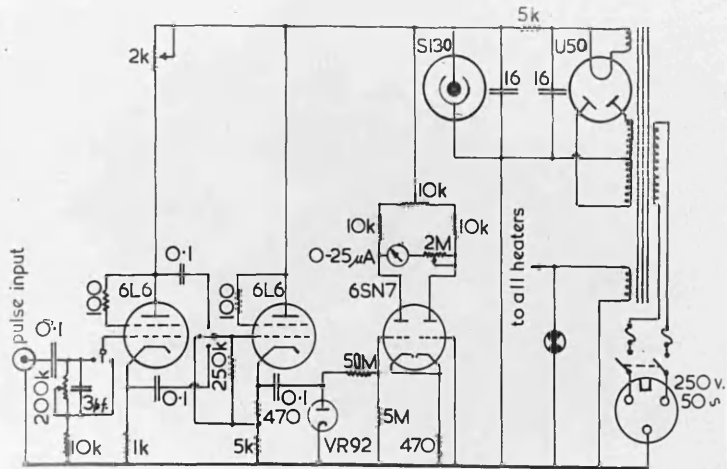
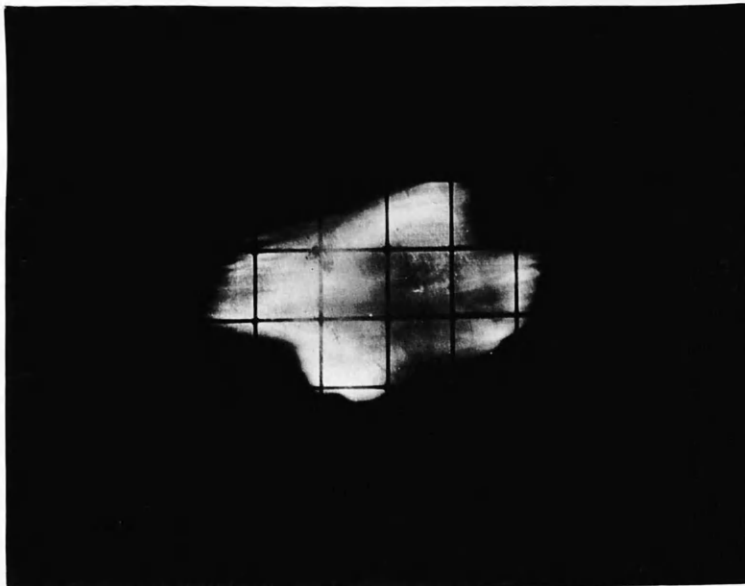


Fig 28 Blackened Perspex-bound Screen

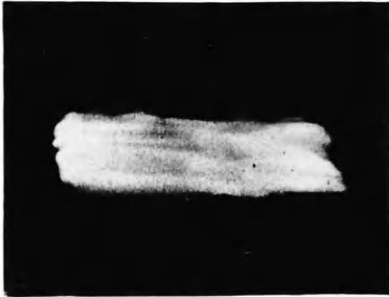


it apparently continues to shrink for a considerable time after hardening. This often leads to complete fracture of the foil foundation. Failure of this kind can be avoided if the coating on the foil is made particularly thin, but thin coatings saturate more rapidly than thicker ones and are therefore undesirable. In actual practice screen-making, which must still be regarded rather more as a craft than a routine process, depends to a large extent on obtaining a compromise between mechanical strength and acceptable intensity linearity.

To make a screen a sheet of foil is first etched in the fashion already described. It is then clamped between the two concentric support rings shown in Fig 30, and trimmed round the edges. A finger is now run lightly round the foil, just inside the periphery, so that the clamping tension is removed and the foil is fairly slack. Coating is done by careful and uniform painting; spraying techniques having been found unsatisfactory with relatively coarse powders and moderately thick coatings. The powder to be used must be prepared in advance, and should be as homogeneous as possible. A convenient method for obtaining a

Fig 29

Life Test of a Silicate-bound Screen.



At Start.



After 3 hours.



After 7 hours.



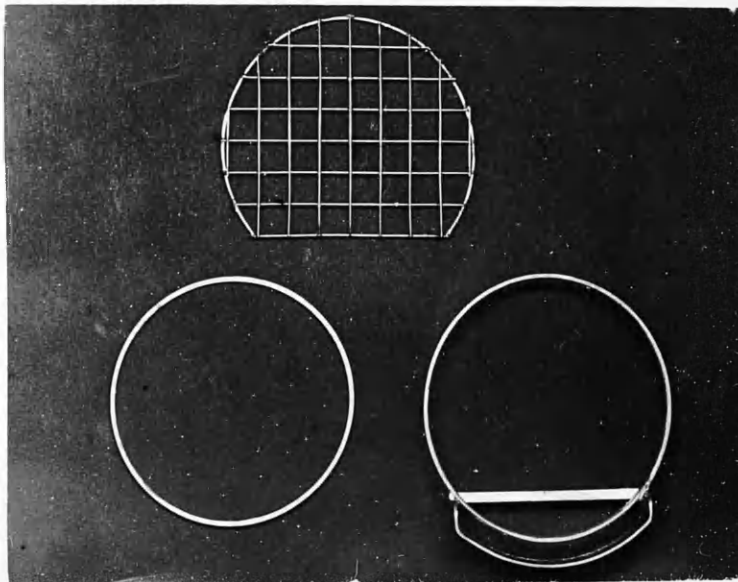
Distortion of the Screen
by bombardment.

In these tests an experimental gun was used, and the mission pattern varied during the test period. Blackening is nevertheless visible, and distortion of the screen surface. The peak voltage was 80 kV, the peak current 250 ma., and there were 50 pulses per second. This is a severe test, as may be seen by comparing the effect shown in Fig 28, where the running time was only 15 minutes.

paste of the right consistency involves filling a small bottle or specimen tube with a quantity of the fluorescent material. To this is added a little of the sodium silicate solution, which should be fairly dilute. Within a few hours it will have soaked through the powder to form a uniform paste. It should be noted that in making this paste it is easier to approach the required consistency slowly from the over-thick condition; for it is very much easier to control dilution than any draining or drying procedure.

The prepared paste is brushed uniformly onto the foil surface, is carefully examined, and then left to dry. Attempts at improving dried or half-dried screens are rarely successful; it therefore pays to prepare both the foil and the paste as carefully as possible, and to acquire a certain degree of skill in the application of the coating. The painted foil should be left in a warm dry place overnight, and will be quite hard the next morning. A brass wire centimetre grid, also shown in Fig 30 may now be placed over the outer clamping ring onto which it is a tight fit. The completed

Fig 30 Fluorescent Screen Mounting



Top: Centimetre Wire Grid

Left: Inner Foil Clamping Ring

Right: Outer Foil Clamping Ring and Base

screen should be left under vacuum for the following night and should readily stand bombardment without serious outgassing on the following day.

111) The Use of Fluorescent Screens

It had originally been hoped that photographic negatives taken from emission patterns on the screen might provide complete information about gun performance. If a sufficient degree of linearity had been obtained the electron distribution might have been determined directly from densitometer readings on the negatives. This has not, however, proved possible, for although the photographic latitude is very large, screen saturation becomes important at negligibly low electron intensities. Fig 31 illustrates these characteristics with a 50:1 difference in exposure for the same emission, and a 10:1 difference in emission for the same exposure. (The negatives were developed to a fairly high degree of contrast; the contrast γ being above unity.) A successful densitometer technique would clearly require tremendous improvement in the screen performance, and this might well involve a modest

Fig 31 Photographic and Silicate Screen Linearities



Emission 50 ma.



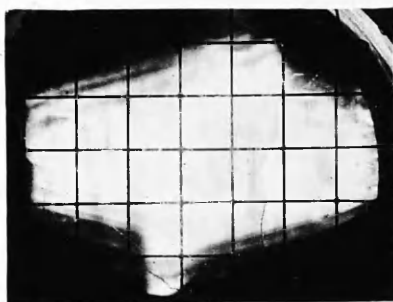
0.1 sec. f 32.



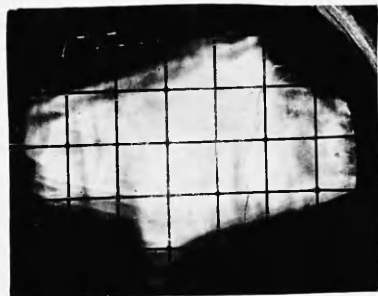
Emission 150 ma.



1.0 sec. f 32.



Emission 500 ma.



5.0 sec. f 32.

The above plates taken
at f 32, 1 sec. exposure.
Equal positive printing.

The above plates taken
for 250 ma. emission.
The positive printing was
compensated.

development programme itself. Such a line of investigation might have been justified if an alternative means for determining electron intensities had not immediately shown greater promise. Probe measurements, in fact, began to yield almost from the beginning the kind of information that fluorescent screens were unable to provide.

It became apparent from the probe measurements that electron distributions and overall pattern shapes were closely related. Guns could therefore be graded fairly accurately, merely by observing the emission patterns, and this saved a great deal of useless current contour plotting with the probe. Moreover, gun geometry is critical, and a barely visible mechanical defect may displace the electron-optical axis of the gun a considerable distance from the intended position. This kind of fault is immediately revealed by the position of the fluorescent pattern on the screen. It is also usually possible, as a result of this observation, to diagnose the cause of the trouble after more critical visual examination of the gun itself.

The present type of screen is therefore useful for the following reasons:

- i) It shows whether a gun is properly aligned or not; and, if not, generally provides a useful pointer to its shortcomings.
- ii) It gives a clear indication, through the shape of the emission pattern, whether the gun is worth testing with the probe unit.
- iii) It is always useful for quick observation of unusual phenomena; and the fact that a photographic record can be taken almost immediately is a valuable additional amenity.

More generally, in its application to gun testing a fluorescent screen is only a rough indicating device; the display it provides is open to interpretation, and must be appreciated within a certain experimental context. It therefore only really becomes useful - it may, in fact, otherwise mislead - when an understanding of the common variations of electron gun performance have already been acquired from the more exact revelations of probe measurement and current contour plotting.

iii) The Probe Unit

It was essential that any satisfactory probe should be readily and accurately movable within an observation area about 8 cm diameter. This requirement was based on an early decision to use the fluorescent screen 8 cm from the point of injection; where the fluorescent pattern is about 7 cm by 4 cm in size, and large enough to be examined critically without being so far away that detail becomes diffused. It was, of course, desirable that the probe and screen should be placed in the same positions, as this would simplify and eliminate ambiguities from correlation.

Movement of the probe had to be controlled from outside the vacuum, and this could easily have led to rather complicated apparatus. A compromise arrangement was therefore adopted, in which the probe motion is not on a truly flat plane normal to the electron-optical axis, but sweeps a spherical surface centred on the axis at a relatively large distance in front of the test position. The probe was, in fact, mounted on a long arm, vacuum-sealed by a short length of telescopic tubing, and freely supported on a gimbal type bearing. The distance between the probe and pivot was made 24 cm,

and an extension on the other side of the pivot, 6 cm long, was added to indicate the probe position on a quarter-scale cartesian grid engraved on a Perspex end plate. Such an arrangement is simple and has also proved reliable and reasonably accurate. There are, however, two inherent geometrical errors, and although they are not, in the applications to be discussed, particularly serious, they are nevertheless worth examining briefly.

It will be seen from Fig 32, in which O is the position of the gun and NP is the probe arm, that the true test plane is normal to OP and passes through Q. When the probe is at the point N, the position on the true test plane to which the reading corresponds is S, and an eccentricity error, ST, is involved. This may easily be determined.

Using the notation of Fig 32:

$$x = b - b \cos \beta = b - \sqrt{b^2 - y^2}.$$

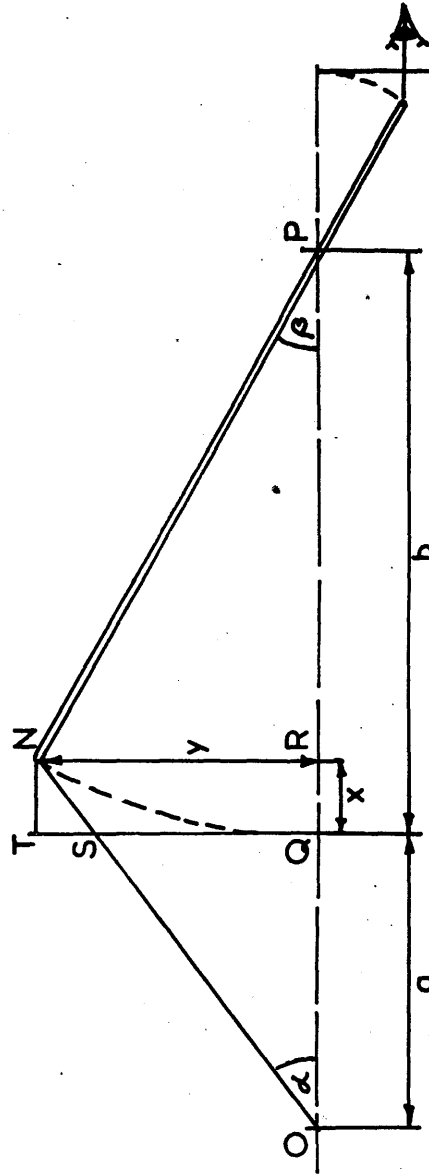
Now $ST:SQ = QR:QO = x:a$; so that the percentage eccentricity error

$$\begin{aligned} &= \frac{100 \ ST}{SQ} = \frac{100x}{a} \\ &= \frac{100(b - \sqrt{b^2 - y^2})}{a} \end{aligned}$$

Substituting the values actually involved, and

Fig 32

Test Probe Geometry



taking y as 3 cm, the eccentricity error is $2\frac{1}{4}$ percent.

In addition to the eccentricity error there is an intensity error caused by the difference between the distances to the gun, OS and ON. The inverse square law applies, and the percentage intensity error, approximately

$$= \frac{200x}{a},$$

or twice the eccentricity error; being, for $y = 3$ cm, 5 percent.

This second error is clearly of greater importance than the first, but the two are fortunately to some extent self-cancelling. In the majority of applications the critical area under examination is only about 2 cm by 3 cm, and within such an area the geometrical errors will be quite unimportant, as the position of the probe can only be defined with an accuracy of about 1 mm.

The design of the probe itself, as opposed to its mounting, was complicated by variation in the angle of incidence of the electrons onto the probe surface. This angle, $\lambda + \theta$ from the axial, which rises to $27\frac{1}{2}^\circ$ for 3 cm eccentricity, revealed very considerable spherical errors in many of the collectors

tested. The trouble seemed to lie, not only in the cosine reduction of the effective probe area, but also, because of the small overall size of the unit, in the effects of a relatively thick-walled aperture plate, which produced further reduction of the effective probe area and a larger source of secondary electrons. Fig 33 demonstrates the extent of the spherical aberration commonly involved; the ball probe having been, in this case, rather hurriedly assembled as a device likely to have at the least better spherical consistency than any other probe previously tested. It was, in fact, so very much superior that it became, with a little refinement, the standard type of head.

Two main improvements were made to the ball probe. The exposed glass on the front of the Kovar seal was aluminized to eliminate the accumulation of electric charge; the coating being scraped away within the immediate vicinity of the lead-through wire. However, this coating very quickly deteriorated under electron bombardment, without causing any perceptible change in the probe performance; it has not, therefore, been replaced. A more important source of trouble

was the ball material itself, for the first ball was made from an $\frac{1}{8}$ in. steel ball-bearing and exhibited curious discontinuities in its response to electrons of different energies - particularly about 20 kV. Various other metals were tested, and aluminium was selected as being by far the most consistent material for this purpose. It is now recognized that the choice may have been rather artificially founded, for the presence of silicone oil in the diffusion pump may have greatly influenced the decision. This oil is inclined to form thin, and possibly mono-molecular films on vacuum surfaces, and would clearly affect the energy-linearity of a probe system on this account.¹ On replacing the silicone by Apiezon mineral oil the probe linearity improved strikingly, although no attempt was now made to confirm the choice of aluminium as a probe and chamber wall material. (It is possible that some of the apparent instability of thoriated filaments may have been connected with silicone poisoning, but this point was not appreciated at the time and cannot be confirmed retrospectively.)

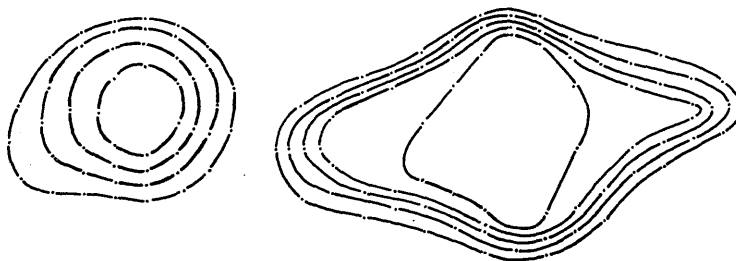
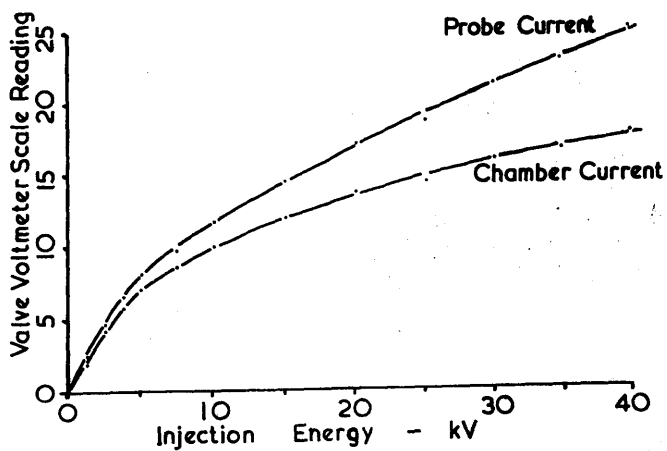
¹

A. Lempicki and A.B. MacFarlane Nature 167
p813 1951

Fig 33

Probe Orientation

The Emission Contour-Plots are for Identical Conditions and the same Gun. Each Plot is taken with the Probe shown immediately above.

Fig 34 Collection Linearity

A fairly rough series of linearity checks was carried out, in which the total chamber and probe currents were measured for different injection voltages and currents. This correlation could never be pressed to exactitude for it soon became evident that the gun emission pattern varies very slightly, in position or shape, with change of the injection voltage and current. This secondary effect cannot readily be taken into account, but it will be seen, from Fig 34, that the probe and chamber current readings are smoothly related, and that consistent relative readings may therefore be expected.

Fig 35 shows various details of the probe unit, and Fig 36 the manner in which it is mounted on the front of the test chamber. It will be noted that the monitoring resistances are both shunted by capacity; this helping to suppress pulse-edge transients incompletely removed by the screening of the earthed anode. Equal R-C time-constants are not convenient because the break-through to the whole chamber is very much greater than to the probe alone. It is, in fact, because of the further coupling between the probe and chamber that a separate switch

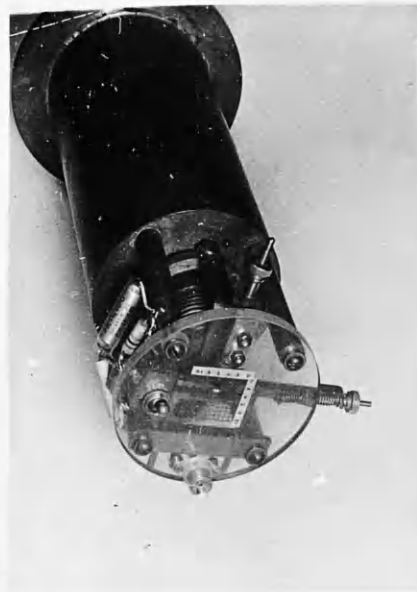
Fig 35 Probe Unit - Details



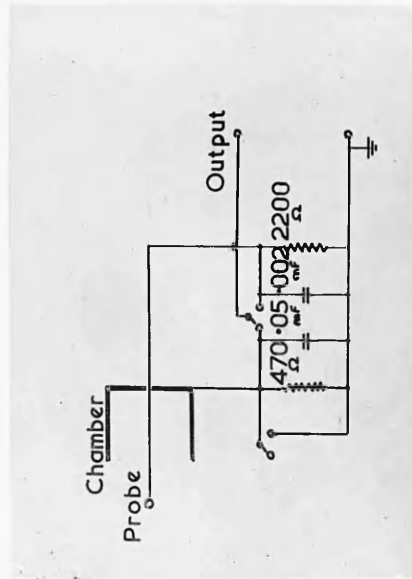
Unit with Aluminium Sleeve withdrawn



Ball Probe



Actuating Mechanism



Circuitry

contact is fitted to earth the chamber whenever the probe is being used. This is essential.

iv) Uses of the Probe

Probe measurements soon made possible a type of gun examination more fundamental and exact than was available by using the fluorescent screen technique. Much that seemed important on the screen was now shown to be quantitatively negligible; while, at the same time, within a critical area, unsuspected and particularly important detail was discovered.

In general, it was found that the fluorescent pattern visible on the screen comprises two contrasting sections, although this contrast is minimized in the visible display. A large striated patch dominates the pattern but is actually of very low intensity, and a smaller high intensity area lies across the striated patch and askew to it. The intensity within the smaller area rises rapidly at its periphery to a broad peak value perhaps ten times greater than that within the low intensity area. The exact shape of the peak varies considerably, and has been found to affect synchrotron performance in a simply predictable manner. It might, in fact, be argued

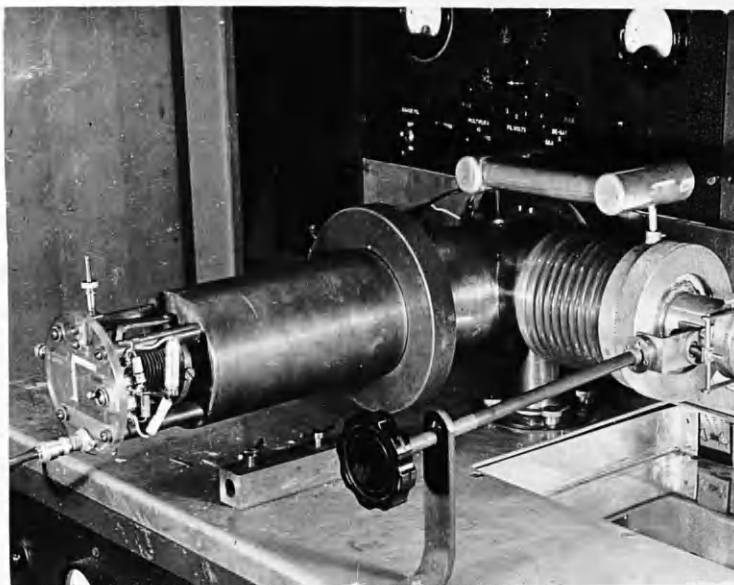


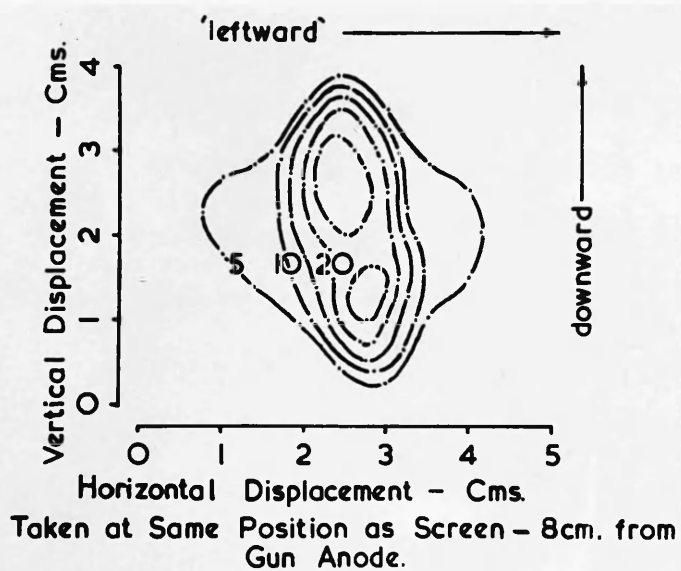
Fig 36 Probe Unit Mounted on
Second Test Chamber

that a probe test on every gun before it is put into use is the most valuable routine check affecting sustained consistency of accelerator output. At this stage it would be anticipatory to discuss the relationship between probe and screen measurements in any great detail, but it is relevant to outline the similarities and contrasts involved. Fig 57 is a typical correlation of the two kinds of result. (It should be noted that, because of the linkage and co-ordinates used the contour plot is always inverted and reversed from left to right.)

v) High Voltage Calibration

One of the purposes of the gun testing unit is to age electron guns to an effective working voltage of 100 kV. This, as we have seen, is less easy to perform with an exponential pulse than with a flat-topped, delay-line formed type of pulse. The fear that the time to initiate breakdown might be long compared with the effective peak width seemed, on the whole, unjustified, for breakdown on the operating synchrotrons has generally occurred close to the front edge of the voltage pulse. It is true that some breakdowns do occur rather later, but they are

Fig 37 Comparison of Data from Screen and Probe Tests



relatively few in number, and delay in breakdown does not appear to depend to any appreciable extent on the amount of the excess voltage. Generally a pulse width of one microsecond has been assumed adequate for establishing breakdown, if it is going to occur. The problem of voltage calibration therefore involves both accurate pulse height and pulse shape determination, so that a nominal peak voltage may be specified where the actual voltage exceeds the test voltage for a period of one microsecond.

Calibration may be approached in three ways: by calculation; by oscillograph measurement; and by sphere-gap testing. The first depends on knowing the pulse rise-time, and the amount of damping imposed on any pulse transformer resonances. The rise-time and pulse shape may be calculated from frequency response and phase-shift measurements; the response of the transformer to a step function of input voltage being then synthesized. The work involved is, however, lengthy, and in the present case seemed unjustified; for the frequency response is predominantly controlled by the main high-frequency resonance of the transformer: a less exact approach, based on a simple L-C-R

equivalent circuit proved adequate. This leads to a pulse-shape equation of the form:

$$V = E e^{-t/T} - E e^{-\omega t/Q} \cos \omega t,$$

where:

E is the voltage to which the pulse-forming condenser is charged, converted to a transformer secondary equivalent,

T is the pulse-forming system time-constant,

ω is the angular velocity of the resonant condition, and

Q is the corresponding amplification.

From the frequency response curve, shown in Fig 38, it is clear that resonance occurs at 150 kc/s, with a Q of 1.42. The load resistance is 53,200 ohms, and the pulse-forming capacity 0.02 mfd. The pulse-shape equation therefore takes the form, for 15 kV on the condenser and a 1 : 9 transformer ratio:

$$V = 135 e^{-0.0940t} - 135 e^{-0.680t} \cos 0.965t.$$

t is in microseconds; and the calculated pulse-shape has been plotted in Fig 39.

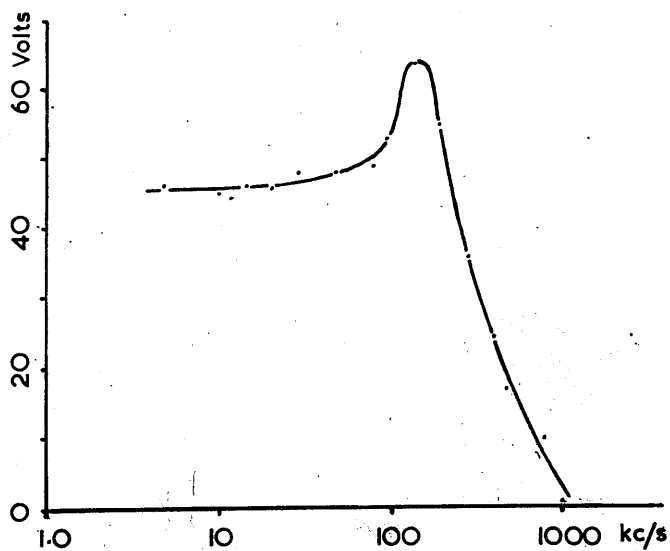


Fig 5B Measured Frequency Response

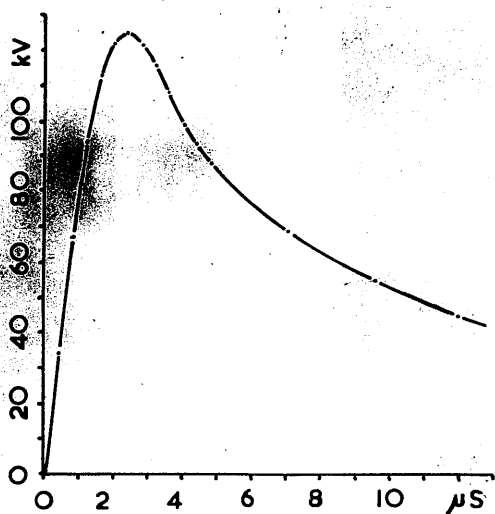


Fig 5C Calculated Pulse Response

It will be seen that the pulse rise-time is about five times as long as the value assumed in the modulator design, but that, because of the resonant overswing, less than ten percent of the ideal peak voltage is lost. Moreover, because of the resonance, the peak is extended in time, and exceeds 100 kV for 2.6 microseconds. In the ideal condition 100 kV would appear on the gun for 3.0 microseconds.

Direct measurement of the pulse voltage is possible by two means; by an oscillograph technique, and with the aid of a sphere-gap. Oscillography is attractive but in this particular case open to some inaccuracy; for a high ratio voltage divider is necessary, and this cannot be properly calibrated under pulse conditions. In order to obtain a 10 volt pulse for application to an oscillograph a 10,000:1 divider ratio is required. This divider system may conveniently be based on the transformer load resistance but should not appear unduly capacitive as any reactance is likely to affect the pulse transformer performance; 3mmfd across the load resistance giving it a 10^0 phase lead at the transformer resonance. It was therefore decided

to make the divider in the form of a long, uniform resistance, without capacity loading, and to correct for the effects of distributed and stray capacities in the bottom, monitoring cell.

The indeterminate capacity can have two effects: it can appear predominantly across the upper parts of the divider, decreasing the divider ratio and tending to differentiate the pulse; or it can appear as shunt capacity to earth, also from the upper parts of the divider, thereby raising the divider ratio and tending to integrate the pulse. In this case the ratio appeared lower than expected, unless a serious error in pulse voltage estimation had occurred, and the pulse rise-time was also appreciably shorter than anticipated. The monitor cell of the divider was therefore capacity loaded until the rise-time and overall shape corresponded as closely as possible with the calculated value. It was now found, by way of confirmation of this manner of adjustment, that the divider measurements agreed closely with the values expected. The divider consists of eight 3 watt carbon resistors joined end to end in a resin bonded laminated canvas tube; the monitoring cell

being placed at the bottom. The eight resistors have a value of 53,200 ohms overall, and the monitoring cell has a resistance of 5.32 ohms across which an 0.15 mfd compensating condenser is fitted. The unit is shown fitted to the modulator pulse transformer in Fig 40.

Sphere-gap testing is carried out with 62.5 mm spheres mounted above and connected across the gun electrodes, so that only the true electrode voltage appears on the gap. The arrangement is such that the 30,000 ohm limiting resistance used in gun ageing also restricts the peak sphere-gap current, thereby extending the useful life of the spheres. The mounting of the gap is shown in Fig 41, where the remotely operated vernier control of the left-hand sphere and the zero-setting adjustment on the right-hand sphere may also be seen.

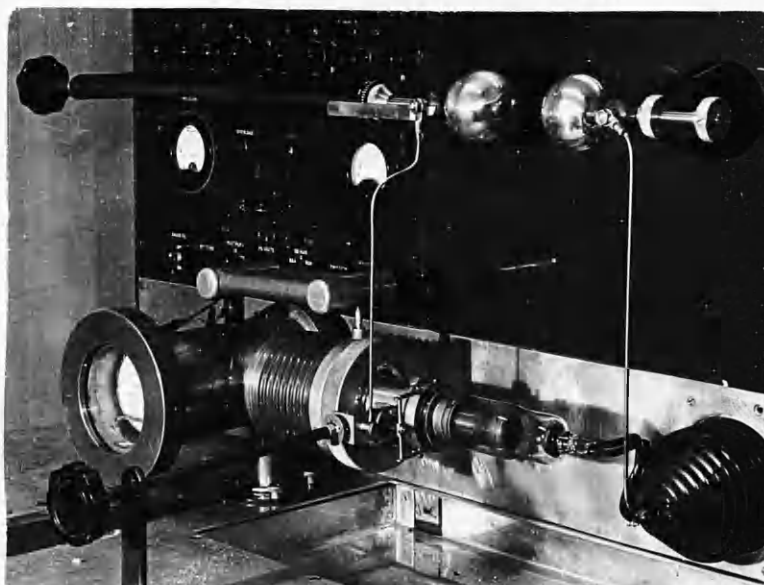
Voltage measurement with the gap has been based on the British Standards Institution calibration for a negative pulse applied asymmetrically to 62.5 mm spheres.¹ Some error was to be expected at the higher

¹ B.S. 358 : 1939 (Amendment PD 224 March 1944)

Fig 40 Pulse Transformer Load and Divider



Fig 41 0.35 cm. Sphere-Gap



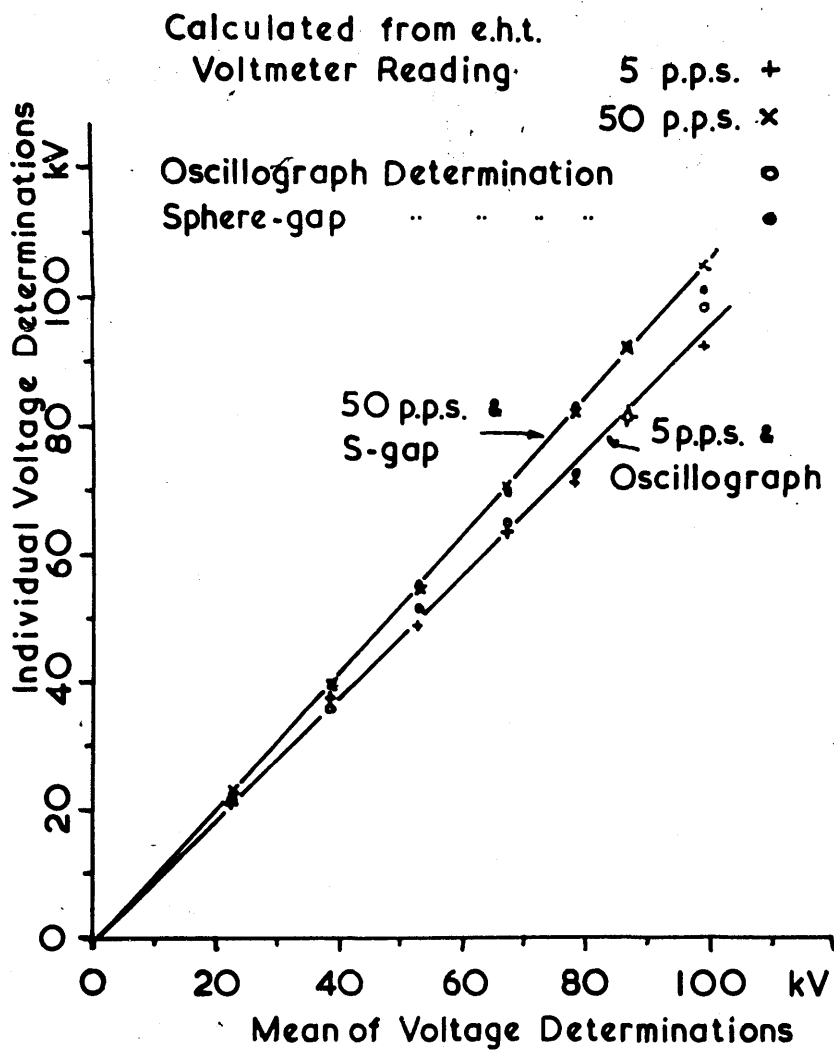
voltages, because the clearances to earth around the gap are considerably less than the calibration specifies, but voltage measurements have nevertheless been found to agree within 10% with all other determinations.

It will be seen from Fig 39 that the peak pulse voltage on the transformer secondary, for 15 kV on the pulse-forming condenser, should be 125 kV. The charge voltage meter is scaled 0-1 for 0-15 kV, so the meter reading is multiplied by 125 to obtain the calculated peak pulse kilovoltage on the transformer secondary. A variation was, however, clearly evident in the meter calibration as the pulse repetition frequency was altered. This was found to depend on the ripple voltage present in the e.h.t. voltage multiplier output. The charge voltmeter does not, of course, record the a.c. component, but this is important in defining the exact charge on the pulse-forming condenser at the moment of triggering. The effect can be reduced by adding to the voltage multiplier reservoir capacity, but in this particular instance space is already so well used that such a method of improvement is quite impracticable.

But it is also possible to alter the charging resistance ($0.5\text{ M}\Omega$ in Fig 26), although this can only be increased with safety until the charging time constant is about half the shortest period between pulses. The value of 0.5 megohm is the best compromise for ripple filtering and accurate charging that the present circuit will allow, and the calibration curves of Fig 42 are based on this value being used.

In correlating the various voltage calibrations it is difficult to decide how much accuracy to allow to each method. One is tempted to favour the sphere-gap measurements because of their remarkable consistency; but it should not be overlooked that the gap geometry has been quite unaltered throughout, whereas adjustments have frequently been made to the charging circuit and the voltage divider. In the end it was therefore decided to average all the determinations and to plot the individual estimations against the average. This reveals close correspondence in pairs of measurement; in the sphere-gap and 50 p.p.s. metering; and in the voltage divider and 5 p.p.s. metering.

Although it might have been interesting to have



Injection gun voltage calibration

examined these inconsistencies more closely, and to have eliminated the effects of ripple, it was not of great importance that the calibration accuracy should be improved. The emission characteristics of Kerst-type electron guns are very little affected by the anode voltage, so that for screen and probe tests an accurate calibration is quite unnecessary. It is of more importance that the voltage should be known fairly precisely when a gun is being aged; but even here, there is such a difference between the performance of a gun in a test chamber and within a synchrotron, and subjected to the vibration and magnetic fields within the annulus, a 10% error in voltage estimation is likely to be eclipsed by the changes in running conditions.

vi) A Note on Ageing

Ageing is normally carried out by running the gun at a voltage where it fairly frequently breaks down. The limit of this frequency is determined by the rate of outgassing that results, and by the pumping speed of the vacuum system. The extent of the outgassing is, however, directly related to the energy

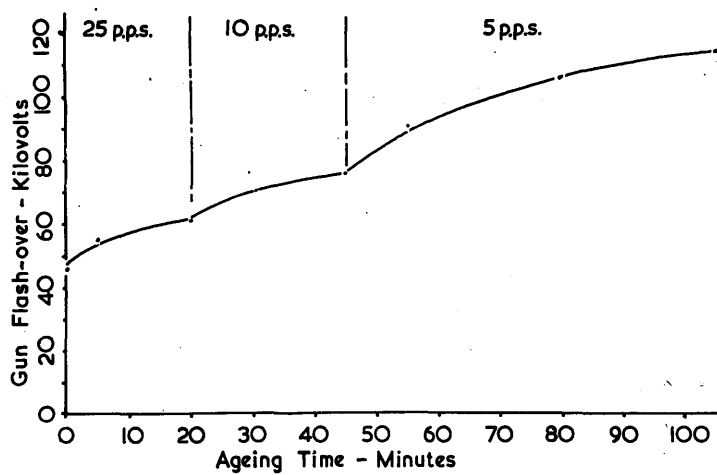
in the breakdown, as well as to the breakdown frequency, and it therefore follows that the gas liberation will be more serious at high voltages than low. Moreover, the release of gas is likely to occur very close to the filament, and momentary resultant changes in pressure are likely to occur in this vicinity which may not be noticed on the ionization gauge. The liquid air trap installed immediately behind the gun position (in the second chamber) is intended to keep these local changes down to a minimum, but it is clear that, although an improvement is certainly evident, complete protection has not been assured; for changes in the thoriation of filaments still occur after some kinds of flash-over which have not produced visible effects in the ionization gauge. The greatest danger is, of course, that a flash-over will produce more gas than can be cleared before the following pulse, and that a sustained recurrence of breakdown will follow. A short series of such breakdowns may do considerable damage to a filament before the surrounding pressure rises sufficiently to trip the vacuum pressure interlock.

To avoid this danger it is important to

relate the pulse repetition frequency to the energy that will appear in a breakdown, whenever one should occur. This has led to an ageing practice in which guns are operated up to a nominal 25 kV at 50 p.p.s.; to about 50 kV at 25 p.p.s.; up to 75 kV at 10 p.p.s.; and at higher voltages at 5 p.p.s. In practice the pulse repetition frequency changes are usually made at the quarter-scale deflection positions on the e.h.t. charge voltmeter. The result is a relatively smooth ageing routine, without at any time subjecting the gun being conditioned to any great danger of recurrent breakdown, and a fairly rapid run up to the operating limit. Fig 43 indicates the manner in which the operating voltage improves with time. This particular curve is perhaps rather better than average, as ageing usually takes nearer three hours to complete: otherwise, however, the curve is characteristic.

Fig 43

Gun Ageing Rate



GUN TESTING

1) Gun Construction

Two basically similar types of electron gun have been tested; the low voltage guns - normally working at about 30-40 kV - for the 30 MeV machine, and the 100 kV guns for the 300 MeV accelerator. Both types of gun are of the conventional type introduced by Kerst, although they differ to some extent in matters of assembly and the means for altering the orientation of the beam.

On the small synchrotron the highest possible injection voltage is determined less by the geometry of the gun electrodes than by the chamber wall, for flash-over to the chemically deposited wall-coating almost invariably sets in at about 80 kV pulse peak voltage. In the 300 MeV machine a similar phenomenon would certainly occur if the filament assembly were not fully shielded from the chamber wall by anode side cheeks incorporated particularly on this account.¹

¹ During development work at Malvern with an unshielded arrangement flash-over occurred regularly at 80 kV peak, using test sections from the 300 MeV machine annulus.

Side shielding has not, however, been provided on the lower voltage guns; for the 30 MeV synchrotron works most satisfactorily at injection voltages about 40 kV, and there is no danger of flash-over to the wall coating at this voltage. The addition of anode side shields makes visual alignment of the gun electrodes more difficult and in any case complicates assembly.

A 30 MeV synchrotron gun is shown in Fig 44. It is predominantly of glass construction, and the only metalwork is associated with the electrodes, their leads and supports; and the telescopic metal tubing, with its flanges and struts, by means of which the gun position may be altered. The glass foundation is convenient in allowing easy adjustment of the electrode structure, and the fact that the electron-optical axis need not be accurately aligned to the glass further simplifies construction and adjustment.

The 100 kV guns are very much more critical in assembly and alignment, are mechanically delicate, and depend on an unsatisfactory means of electron-optical distortion for one adjustment of the electron

Fig 44 30 MeV Synchrotron Gun

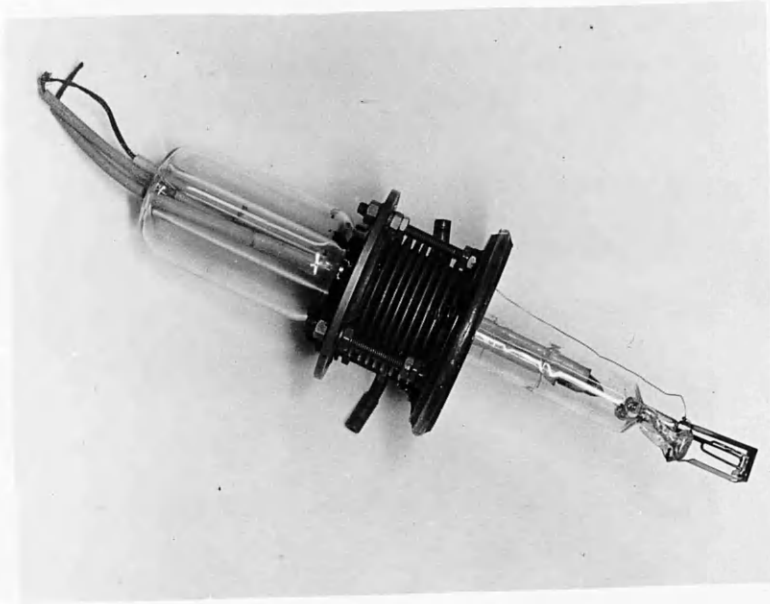
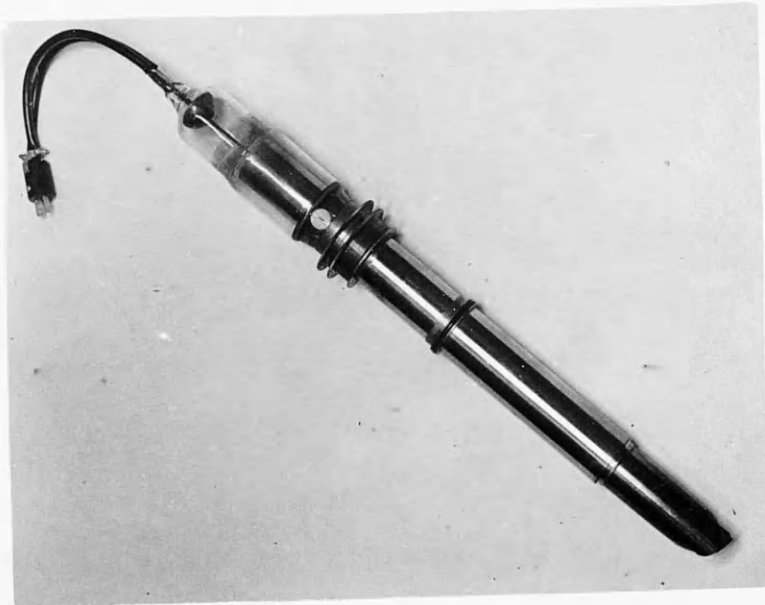


Fig 45 300 MeV Synchrotron Gun

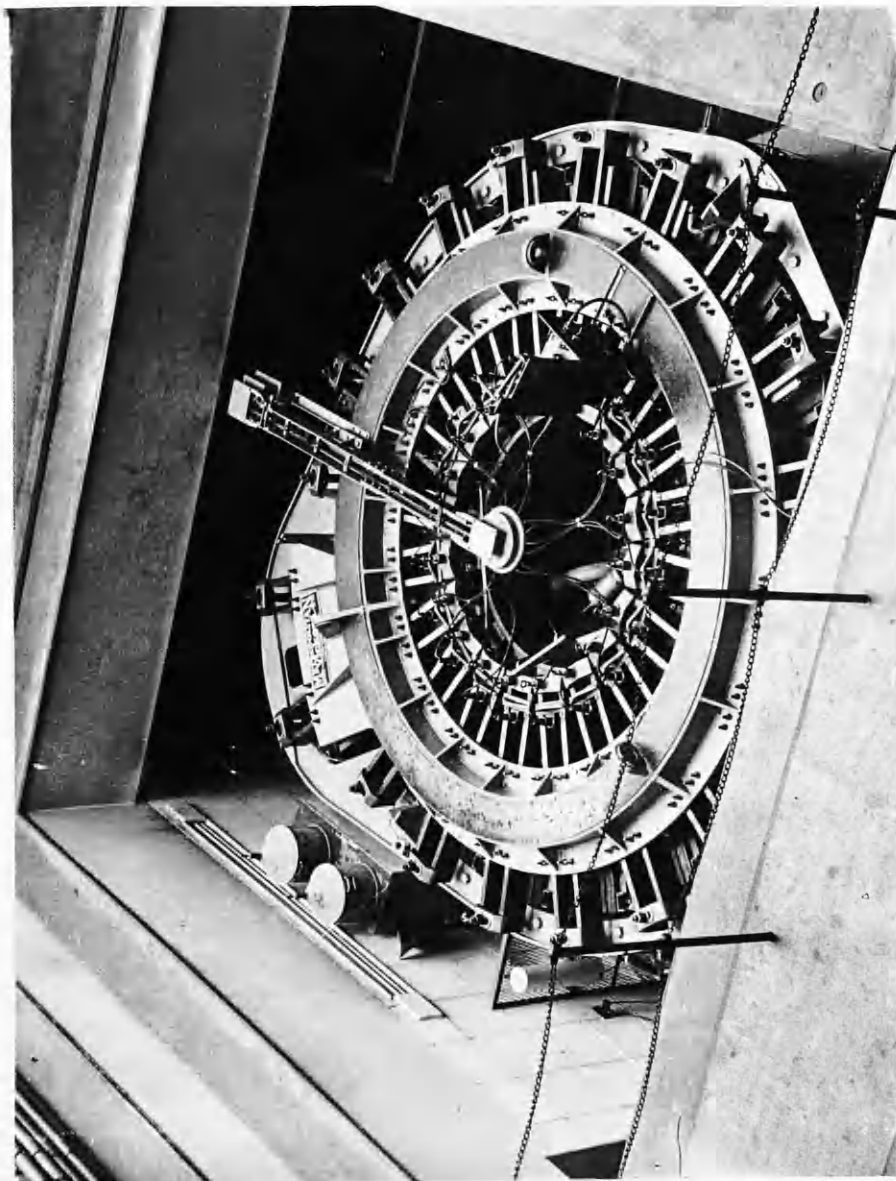


beam direction. They are predominantly metal, and are constructed to precision tolerances almost throughout; so that there is little scope for developmental modification without recourse to a fairly comprehensive re-design. They are also very much more difficult to align than the low voltage guns, for the position of the injection axis relative to the body of the gun is now critical.

A 100 kV gun is shown in Fig 45. It is mounted inside the equilibrium orbit, as all access to the vacuum chamber of the 300 MeV synchrotron is from the centre of the machine, as may be gathered from the illustration of the accelerator in Fig 46. The gun itself is represented schematically in Fig 47. It will be seen that the filament assembly is supported on a glass or soapstone column mounted a little behind the actual gun electrodes, and that from this assembly two open rods lead down the centre of the gun body to the glass insulator at the other end. The insulator, filament assembly, and support column are collectively mounted on an inner stainless

Fig 46

Glasgow 300 MeV Synchrotron



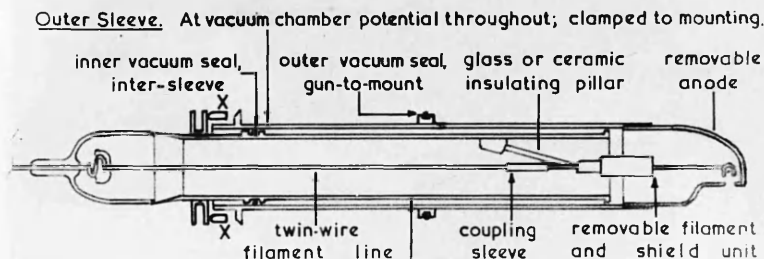
steel tube which, near the metal-to-glass seal, carries two rings surrounding the tube and riding on it on fine threads. Outside this stainless steel tube is a second similar tube which carries the removable anode at one end and a flange for locating the gun at the other, close to the two adjustable rings.

The simpler gun mounting, which is used on the gun testing unit, is shown in Fig 48. The gun is inserted through the aperture at the end of the mounting and is thrust forward until the outer flange, on the outer stainless steel sleeve, lies against the circular step in the mounting mouth. Three radially disposed screws slightly away from the step are then tightened until they bear on the bevelled face of the gun flange. On evacuating the test chamber the inner sleeve is thrust inward by the outside pressure until the nearer of the two adjustable rings (the second is only for locking purposes) is restrained by the two rocker arms on the gun mounting. In the simpler mounting these arms are clearly visible, the tie-bar between them, and the screwed rod by which they may be moved are also visible. The Tufnol

Fig 47

100 kV Gun Components

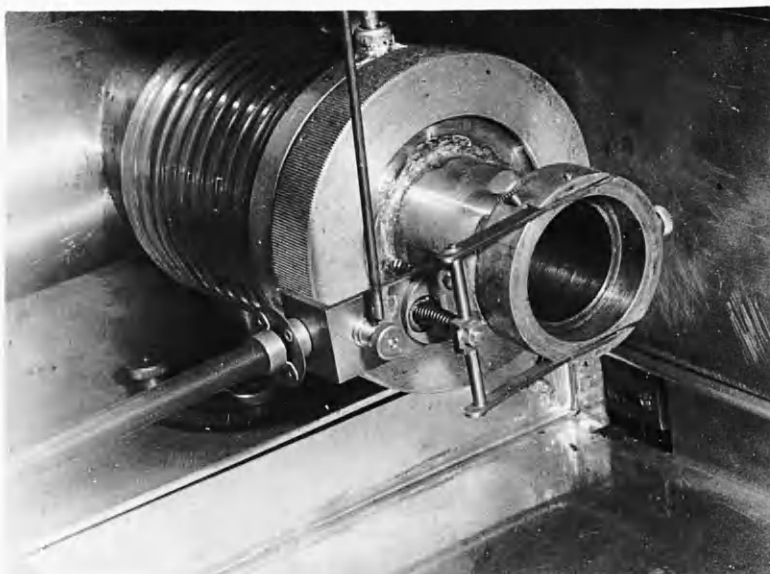
SCHEMATIC SECTION - Not to Scale



Inner Sleeve. This carries all the high voltage components. It is free to slide within the outer sleeve but is held against the two bearers, XX, by atmospheric pressure. The position of the shield and filament relative to the anode aperture, and hence the angle of injection, may be altered by moving the bearers.

Fig 48

Test Mounting for 100 kV Gun



rod on the lefthand side of the figure allows the arms to be moved while the gun is being pulsed.

Fig 49 shows the more complicated mounting used on the 300 MeV synchrotron. This unit, designed by the A.E.R.E. Accelerators Group, is necessarily compact, for the mounting is carried on a vacuum chamber port placed between two of the twenty betatron bars, which carry the betatron flux during the initial part of the magnetization cycle. These bars are, at their closest points, only $5\frac{1}{2}$ -6in apart.

It will be seen from the labelled diagram of the gun mounting, in Fig 50, that it contains three main components. The second sub-platform corresponds in function to the recessed mouth and rocker arms in the test chamber gun mounting. In this case, however, the sub-platform is arranged to rotate about a radial axis on the first sub-platform, so that the electron beam may be directed above or below the equilibrium orbit if this should be required. The first sub-platform is itself free to move radially inward or outward on pillars carried on the main platform which is rigidly secured to the end of the vacuum chamber port. It is therefore also possible to vary the radial position of

Gun Mounting on 300 MeV Synchrotron



Fig 49 Unit in Position

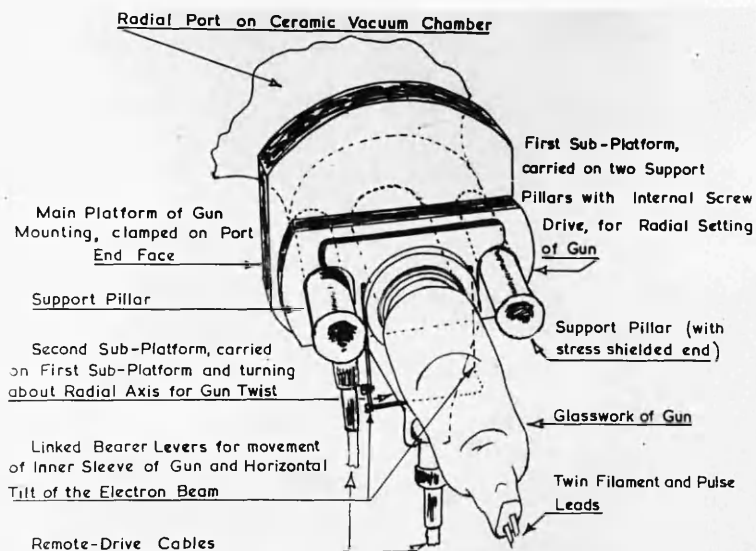


Fig 50 Mounting Components

injection into the annulus.

The three variables provided in this mounting are remotely adjustable by means of electric motor and flexible cable drives from a control box fitted some short distance underneath the gun mounting. Potentiometer and meter position indicators are connected with the remote operating positions in the synchrotron control equipment.

11) Electron Optics

The performance of the electron guns is not amenable to calculation, for both the accelerating gap and the helical filament behave in complex manners.

The anode may be treated, very approximately, as a simple aperture with a field gradient on the filament side but none on the other; the gradient being the accelerating voltage divided by the anode-to-shield separation, and the focal length of the lens $4V/v$; where V is the accelerating voltage and v the voltage gradient. This indicates a focal length about four times the anode-to-shield separation, and suggests that the electron beam will always leave the anode divergently, since the filament is invariably

closer to the mouth of the shield than is the anode. A rough comparison with the conditions required for rectilinear flow also suggests that the beam will be divergent.

The helical filament further complicates analysis by making the emission source indefinite. It is reasonable to assume that the exposed parts of the filament winding will emit more intensely than the considerably screened parts nearer to the back of the shield, and it does, in fact, appear that emission is restricted to the filament surface on the edge of the accelerating field: what is not so simply understood is that overall accelerator performance has, in some instances, been affected by the phase of the a.c. filament supply; a condition suggesting that the emission conditions are significantly altered by the instantaneous heating current and possibly its time-derivatives.¹ This curious effect has not been observed on either of the Glasgow machines, and is certainly difficult to account for: it is, however, only one of several strange phenomena associated with

¹ Prof. E.M. McMillan, of the University of California, Berkeley, California, discussed this effect on a visit to Glasgow University in 1949. Verbal reports of the same kind have been received from other sources.

this kind of gun cathode.

The most important, and also the most obvious factor affecting filament performance is the temperature gradient from end to end, for this is one of the fundamental constraining influences on the emission pattern. Only a relatively short length of the filament near to the centre is likely to emit an appreciable number of electrons, and in the extreme condition it is possible that emission may occur from one hot spot on the outermost surface of the thermally central turn. The last possibility gained favour after it was found that extreme changes in the emission pattern sometimes followed a flash-over to the emitting area: it seemed unlikely that such extensive damage to the emitting source would occur if the emission were taking place from a number of adjacent turns.

A more striking effect suggestive of single-turn emission was occasionally to be found in a particular type of faulty gun characteristic. On the assumption that single-turn emission is normal, emission from two adjacent turns might be expected to lead to two similar and overlapping patterns separated by an amount primarily related to the filament winding pitch.

This kind of distribution has actually been observed on a few occasions, and it is interesting to note that machines fitted with guns having this peculiarity do not, in fact, work well. There are, however, two peak output positions separated by an angular rotation of the gun about a radial axis. A photograph of a dual emission pattern is unfortunately not available.

The normal type of emission pattern is still open to fairly wide variation, but no serious effort has yet been made to correlate the emission characteristics with the electron-optical aspects of gun design. An attempt to determine the beam spread by taking fluorescent screen photographs at 2cm intervals along the injection axis has nevertheless been particularly instructive, for the derived results demonstrate that the beam is neither simply divergent nor emitted from a single turn. The five pattern photographs, taken for a particularly good gun, are shown in Fig 51, while the derived results, based on the height and width of the high intensity skewed core, are shown in Fig 52.

The most surprising indication of these tests is the apparent length of emitting filament. In this case the useful length appears to be about 9mm, and an unexpected

Fig 51 Beam Spread Measurements

Distances:

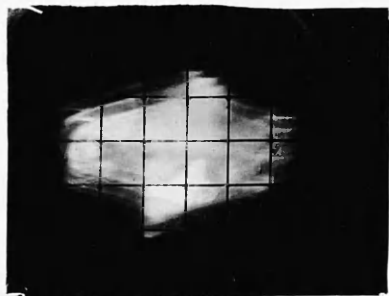
6 cm

2 cm

8 cm

4 cm

10 cm

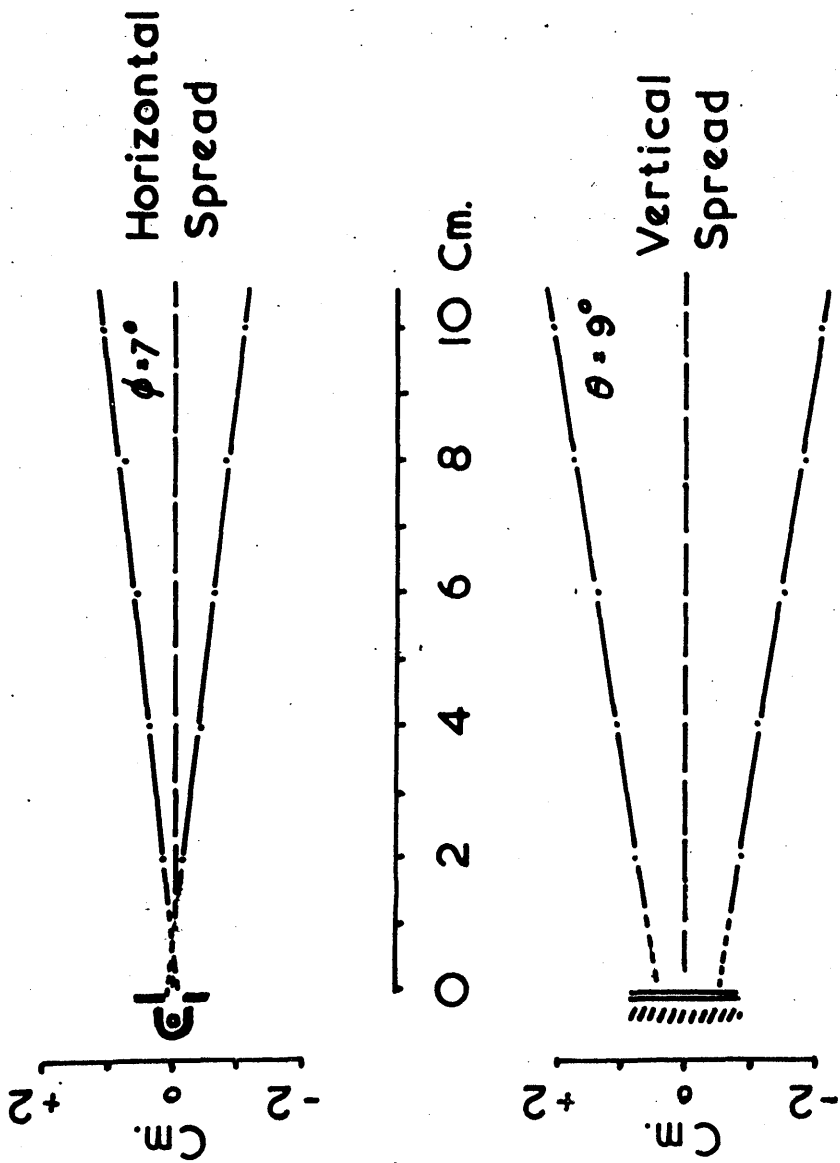


correlation is evident linking this length, the filament winding pitch, and the number of striations in the larger, secondary part of the emission pattern. The filament winding pitch is approximately 1mm; so that, although the striated pattern is irregularly distributed and sometimes poorly defined, the fact that about 8-10 line components are involved is hardly coincidental.

If the electron source is larger than a single turn the occasional dual pattern already discussed cannot be so easily explained. But if a flash-over to the emitting area does extreme damage in the immediate vicinity of the arc, driving all the surface thorium from the winding, it is probable that emission will subsequently occur from more distant parts of the winding; the whole filament being run a little hotter to bring the fringes up to emitting temperature. Such an effect following a flash-over to the centre of the winding might well produce the kind of effect already observed: it would also help to explain the reduced output available from this kind of gun.

.

Fig 52 Derived Beam Spread Results



The geometrical alignment of the gun electrodes is in some respects extremely critical. In particular, the filament must be exactly centred between the cheeks of the shield if the electron beam is to emerge along the intended axis. The emitted electrons, following the lines of force in the accelerating gap, tend to be injected in the same direction as the filament eccentricity, and may often be very appreciably displaced on account of a barely perceptible misalignment of the filament.

The critical nature of the filament and shield positioning clearly demands high mechanical stability in the electrode system. The fact that the filament and shield both operate at high temperatures might be thought an additional problem but relatively little trouble has been directly attributable to this fact. (A good deal of minor trouble in the 100 kV guns has been apparently caused by a combination of temperature change and vibration from the magnet pulsing, but this has usually been confined to clamps and resilient couplings remote from the electrode assembly.) The most serious cause of filament instability, provided the initial filament processing has been satisfactorily carried out, is

the cumulative effect of small amplitude vibration, particularly between the two filament supports. This motion imposes alternating stresses on the filament, which, because of its plasticity at running temperature, will be inelastically strained, and permanently deformed. Gun reliability is therefore primarily dependent on two requirements: on the filament being exactly aligned within the shield, and on its ends being securely attached to inelastic support pillars.

The geometry of the accelerating gap is much less critical, presumably on account of the axial length of the lens and its nearness to the emitting source. The anode, indeed, has very little effect on the beam, which tends to emerge normally from the plane of the mouth of the shield, unless the filament is asymmetrically disposed within the shield. On this account relative movement of the shield and anode has proved only partially successful as a means for beam shifting. The efficacy of the method varies to some extent with the relative width of the anode slit and the shield mouth, but the beam shift is generally small - rather less than 10° overall - and masking of the emission pattern by the nearer anode tongue rapidly occurs. This effect can be

misleading when a gun is being adjusted in an accelerator, for it may suggest that an optimum setting has been reached when anode masking introduces a false symmetry onto what is really only a region of improvement. This danger is fortunately reduced in the case of the 300 MeV synchrotron, by the fact that the injection pulse shape alters slightly - in differentiation spikes - as masking begins.

The most serious argument against the lens distorting method of beam shifting is certainly, however, its limited range; for the critical importance of the filament position makes the initial position of the injection axis difficult to control, and any beam shifting system should be able to accommodate the considerable initial error which may be involved. The 10^0 overall shift provided by lens distortion is quite inadequate.

There are two rather simple geometrical factors which have tended to increase the initial error, and which deserve passing mention. The lens itself is strictly asymmetrical, for the two anode tongues are appreciably different in shape. An attempt to

improve the symmetry by adding a flange to one of the anode tongues, as shown in Fig 53, was quickly abandoned because of the extreme danger to the filament and shield whenever the tight-fitting anode was removed or replaced. This was no great disadvantage, for it was relatively easy to correct the asymmetry by another means. The second source of trouble was simpler in nature for it had nothing to do with the gun design: it was only a matter of assembly. It was found that there was a general tendency for the shield, when mounted, to lie with the plane of the mouth not truly radial; the normal line of the beam inclining toward rather than being parallel with the equilibrium orbit, as shown in Fig 54.

Both the anode asymmetry and the misalignment of the shield produce errors which displace the beam toward the orbit, and the overall effect is usually greater than the lens distorting beam shift will accommodate. To correct the overall error it has now become a matter of policy to twist the mouth of the shield deliberately away from the equilibrium orbit, so that the injection axis is slightly away from rather than parallel to it. Some 3° - 5°

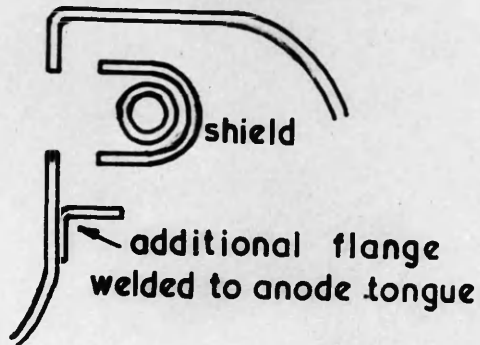


Fig 53 Additional Anode Flange for 100 kV Gun

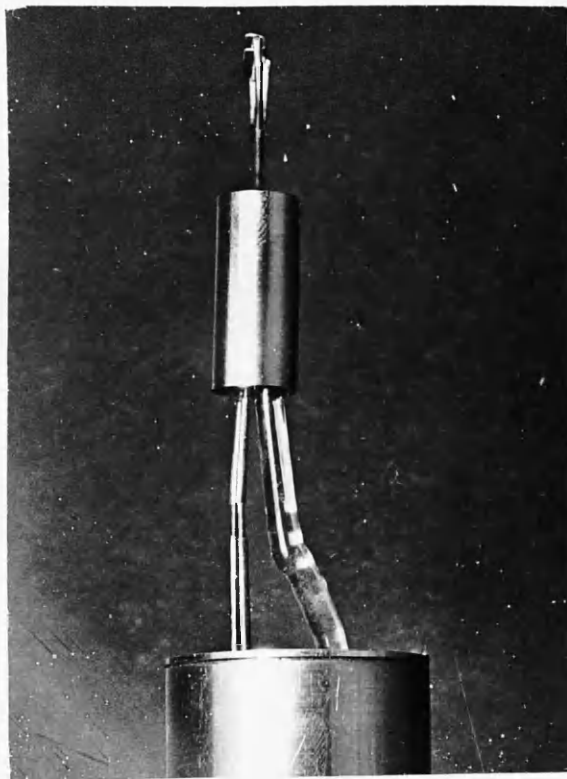


Fig 54 Assembly Error in 100 kV Gun

compensation is usually enough, if the filament is accurately placed within the shield, and this angle can be adequately accurately judged by eye during the assembly.

These alignment problems are, of course, peculiar to the high voltage type of gun, for the lower voltage model may be swung freely over appreciably wider angles. The variable lens method of beam shifting has singularly little to recommend it: it is a precious and rather ineffectual technique which would be well dispensed with in any new design of gun. It is undesirable not simply because of the limited beam movement it allows but also because this limitation imposes too stringent limits on the acceptable geometry of the gun. Moreover, from an experimental standpoint, the variation of the emission pattern with change of the injection axis is a most undesirable feature. An indication of the range of movement, of the extent of the masking and pattern change which occur at the ends of the movement, is provided in the series of tests collected together in Fig 55. Position 12 in the series corresponds approximately with the centre of the overall beam motion.

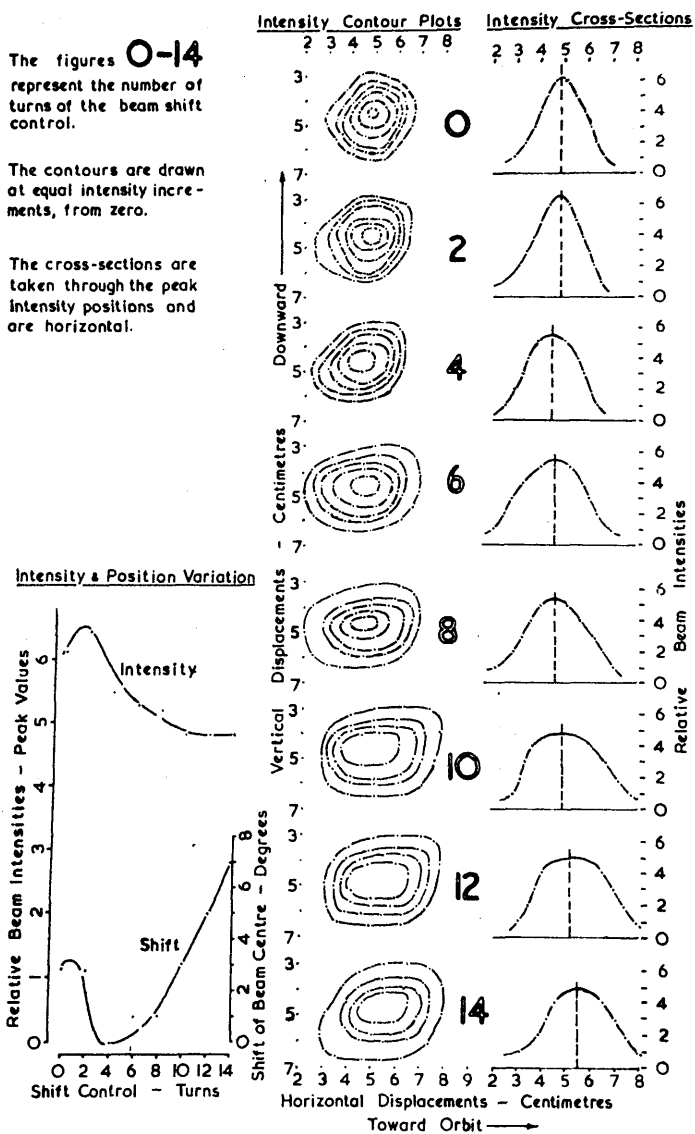
Fig 55

100 kV Gun Tilt Analysis

The figures **0-14** represent the number of turns of the beam shift control.

The contours are drawn at equal intensity increments, from zero.

The cross-sections are taken through the peak intensity positions and are horizontal.



111) Beam Pattern Observations

The relative merits of screen and probe testing have already been discussed, and some comparative results have been quoted, but a satisfactory correlation between the observed gun characteristics and the related synchrotron performance has not yet been considered; although the final usefulness of gun testing must depend upon such a correlation being established.

Much of the value of the curves relating machine output to gun twist and tilt, in Figs 14, 16, and 17, has been lost because the electron distribution from the guns used for these tests was unknown. But such information generally confirms, although it may also to some extent complicate, the impression already gained of accelerator performance. Figs 56 and 57 are a case in point. Fig 56 is a contour plot of the emission density from a slightly unusual 100 kV gun prior to its installation in the 300 MeV machine. The gun is unusual on account of the complex configuration of the emission peak, represented also in the two distribution cross-sections, X-X and Y-Y. Fig 57 is a record of the variation of the

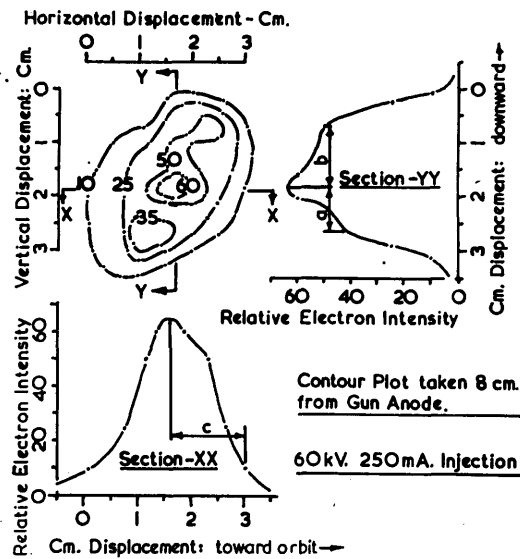


Fig 56 Emission Contour Plot for 100 kV Gun

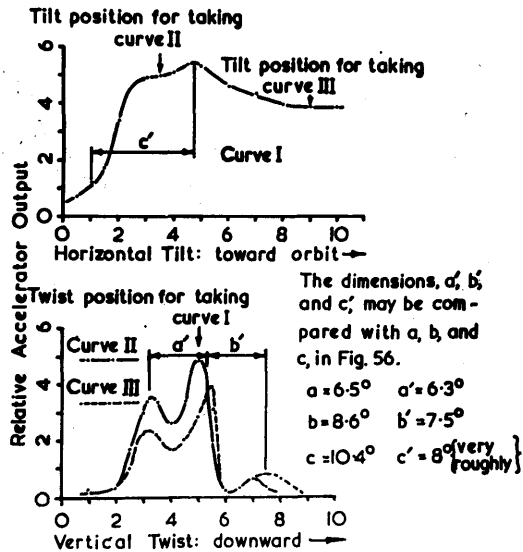


Fig 57 Tilt position for taking curve II and Tilt position for taking curve III

synchrotron output with gun twist and tilt. The variation of the output for rotation of the gun about a radial axis will be seen to correspond strikingly - and also strangely exaggeratedly - with the vertical cross-section of the electron distribution, Y-Y. A similar kind of agreement may be observed between the horizontal tilt of the beam and the cross-section X-X, although here a very obvious non-linearity is introduced. This secondary effect is, however, to be expected, for the abscissa of the two curves represent different and complexly related variables; one being a mechanical displacement, the other an electron displacement. That the two are not directly related has already been indicated in Fig 55.

It is the contrast between the vertical cross-section of the beam and the radial twist curve that is most interesting in this particular comparison, for the extent of the exaggeration of the beam characteristics in the machine performance is unexpected and difficult to explain. But it is quite possible that the important phenomena are not the three isolated peak-output conditions, but rather the low-output troughs that separate them.

For the existence of double electron beams has already been observed on several machines, including the 30 MeV synchrotron at Glasgow, and it is possible that the troughs in the performance curve derive from the interaction of two initially comparable electron beams.¹ A further relevant consideration is the height and width of the annulus, as output in other machines has been found to be critically dependent on these dimensions.² The critical annular dimensions are usually appreciably smaller than the actual annulus sizes involved, and this has certainly proved to be the case on the 300 MeV Glasgow synchrotron, so there is little danger of geometrical restrictions affecting the machine when it is properly aligned.³ However, the low-output troughs in the gun twist characteristic represent abnormal conditions of a vertically asymmetrical nature. It is therefore possible that in such circumstances the critical annulus dimensions approach more closely, and

¹ E.D.Courant Journal of Applied Physics 20 p611 1949
J.D.Lawson Nature 165 p109 1950

² Elder, Langmuir, and Pollock Rev. of Scientific Instruments 19 p607 1948
J.D.Lawson A.E.R.E. Memorandum E1/M2 1949

³ W. MacFarlane et. al. Glasgow 1955 (Unpublished)

possibly exceed the physical limits of the annulus. It is not, with the present amount of information, advisable to speculate further: the important point is not so much to explain the effect as to illustrate that phenomena of this kind may be observed after emission pattern tests have been completed, but are otherwise unlikely to be appreciated.

iv) The General Correlation of Gun and Machine Performances

Although the results contained in Figs 56 and 57 are to some extent unusual they confirm that gun and machine performances are closely related. They also suggest that the peak machine output is directly related to the injected electron intensity within the acceptance angle of the machine. Nevertheless, such a relationship cannot apply unreservedly, for there will certainly be a space-charge limitation on the number of admissible electrons. This effect is, indeed, clearly evident in the betatron characteristic relating machine output to gun emission, which usually passes through a maximum when the emission pulse current is a few hundreds of milliamperes. It does, however, seem that space-charge limitation is an indirect rather than a direct influence on machine performance; that

the solid angle within which the greater part of the beam is concentrated is the more important consideration. It may be seen, for example, that the output obtainable with the clearly broader beamed gun in the 30 MeV synchrotron tests of Fig 19 is appreciably less than that for the narrow beamed gun used in the tests of Fig 14, although the later tests were carried out with the resonator in a better position. Here the geometry is otherwise unaltered and the space charge limitation should be the same. It must therefore be assumed that the ratio of accepted to rejected electrons from the later gun was low, and that this ratio is an important factor in the overall performance determination. When it is low a marked improvement in machine performance may be expected irrespective of the space-charge restriction.

Much will obviously depend on the solid angle within which electrons may be accepted into useful orbits, and if it is small there is clearly a case for improving gun optics. This, it should be recalled, runs against the original desire to design a relatively broad-beamed gun which could be inserted easily, without great anxiety about alignment. It would seem that

ease of alignment may be too injurious to the overall performance, although this will clearly depend on the size of the acceptance angle.

The only acceptance angle that can be calculated with any certainty is itself an artificial one, for two reasons. In the first place it is difficult to define 'acceptance'; for the initially important electrons may be vastly more numerous than those which complete the acceleration process. Others may be involved in induction and electrostatic phenomena in ways that have already been discussed. The second artificiality arises from considering a single electron in a guide-field of constant n -value.

We have seen that, for the radial and vertical oscillations:

$$\begin{aligned}\Omega_{\text{radial}} &= \omega \sqrt{1 - n}, \quad \text{and} \\ \Omega_{\text{vertical}} &= \omega \sqrt{n}.\end{aligned}$$

We have also seen that the oscillation amplitude, A , is proportional to $1/\sqrt{H}$, where H is the guide-field intensity. The period of oscillation will be of the order of, or less than, 0.1 microsecond, within which time the change of field in a 50 c/s magnet system may be neglected. The oscillation decrement may therefore be neglected, and

if we choose our azimuthal references appropriately we may write,

$$d = A \sin \omega t,$$

where d is the displacement from the equilibrium orbit, and A is the oscillation amplitude, which for this examination is assumed the largest possible, and not merely that defined by the positions of the gun and target; it will be defined either by the physical boundaries of the annulus, such as the resonator walls in the 30 MeV machine; or by the edge of the focussing field, where $n=0$ or ± 1 , in the larger machine. This last stipulation makes the following calculation for the larger machine even more artificial, for it assumes a constant n -value throughout the whole of the stable region.

It is convenient to consider the vertical oscillation first, since it is also the simpler. In this case, where injection occurs in the equatorial plane, the acceptance angle may be taken as that contained by the maximum positive and negative slopes of the largest possible vertical oscillation. Differentiating the oscillatory function and taking the vector sum of this result and the orbital velocity, if the total acceptance angle = 2θ ,

$$\theta = \tan^{-1} \frac{A_{\text{ann}} \sqrt{n}}{w r},$$

and the total acceptance angle, 2θ ,

$$= \frac{180 h \sqrt{n}}{r} \text{ degrees,}$$

where h is the total useful height of the annulus, and r is the stable orbit radius.

For the 30 MeV machine, $h = 3\text{cm}$, $r = 10\text{cm}$, and the average n -value may be taken as 0.6. From these values $\theta = 6.6^\circ$. In the case of the 300 MeV machine, however, h is limited only by the focussing field geometry and may be taken as 5cm; the n -value being assumed 0.7, and $r = 125\text{cm}$. From these values $\theta = 0.96^\circ$; a result indicating a considerable difference in proportionality between the two accelerators.

The radial oscillation is more complicated than the vertical one, because the centre of the oscillation and the point of injection are no longer co-incident. It is still, however, true, that the ~~maximum~~ positive and negative slopes of the largest possible oscillation represent the limits of the acceptance angle for injection at the equilibrium orbit radius. For this case,

$$2\phi_0 = \frac{180 w \sqrt{1 - n}}{r} \text{ degrees; where } w \text{ is the total useful width of the annulus.}$$

At the outside limits of the oscillation the acceptance angle is still determined by the angle between the positive and negative slopes, but as these are both zero the acceptance angle is also zero. The acceptance angle is, in fact, a cosine function of the displacement of the point of injection from the equilibrium orbit. The general equation for this angle, ϕ , may therefore be written:

$$\phi = \phi_0 \cos \frac{\pi d}{w}.$$

Again considering the 30 MeV machine, and assuming the same values as previously, but in addition that $w = 4\text{cm}$, $\phi_0 = 7.4^\circ$. In the case of the larger machine a less approximate estimation alone is possible. In this machine the n -value is a function of the excitation, and the betatron orbit is also changing appreciably at the time of injection. Moreover, pole-face coils have been added to correct some of these effects, but they are set empirically for maximum output rather than adjusted for maximum correction. It is therefore quite impossible to select representative values to insert in the above equation. However, if the n -value is taken as 0.6 over an annular width of

12cm, a reasonable indication of the acceptance condition may be expected. The resultant estimate of ϕ_0 is 1.7° . The variation of the overall acceptance angle (2ϕ) with the displacement of the electron gun from the stable orbit is represented, on the basis of the above calculations of ϕ_0 , for both accelerators, in Fig 58.

.

Although the acceptance angles plotted in Fig 58 are to a very large extent artificial in character, there is enough difference between the two curves for this to be reflected in the behaviour of the two synchrotrons. For although gun performance has never been a highly critical factor in operation of the 30 MeV machine it has always been a central consideration in running the 300 MeV machine. The contrast is certainly accentuated by the secondary difference in the means whereby horizontal shift of the beam is brought about; but for vertical shift a mechanical rotation is common to both machines, and here the contrast is still conspicuous. In the case of the 300 MeV machine there is often imperceptible difference

between the vertical beam cross-section and the gun twist sensitivity curve; as shown in Fig 59. It is probable that a similar correspondence relates the horizontal cross-section and the gun tilt curve, but this cannot be successfully established because the abscissa of the two curves are dimensionally different and complexly related.¹ For the lower energy machine, however, these close correspondences, which indicate a narrow acceptance angle, are markedly reduced: irregularities within the gun pattern are fairly completely concealed in what would appear to be fairly wide-angle acceptance conditions. (It will be recalled that within the useful annulus defined by the walls of the r.f. resonator, the n -value does not approach closely to unity, whereas in the 300 MeV machine the useful annulus is defined - or must be assumed defined - by the physical limits of the focussing field. It may also be noted that the curious variations in the curves of Fig 14, which are not evident in any other twist and tilt tests on the low energy machine, are likely to result from some

1

See page 95.

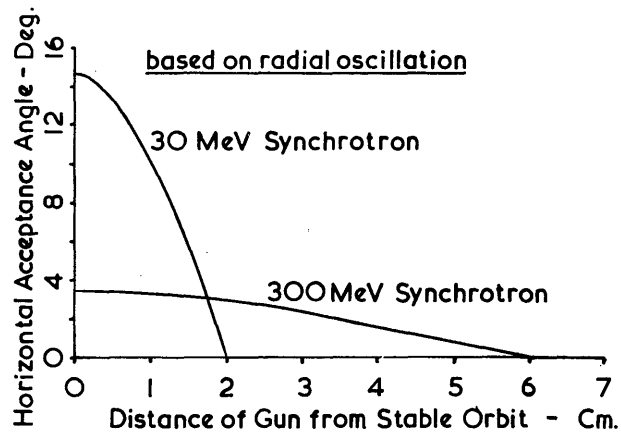
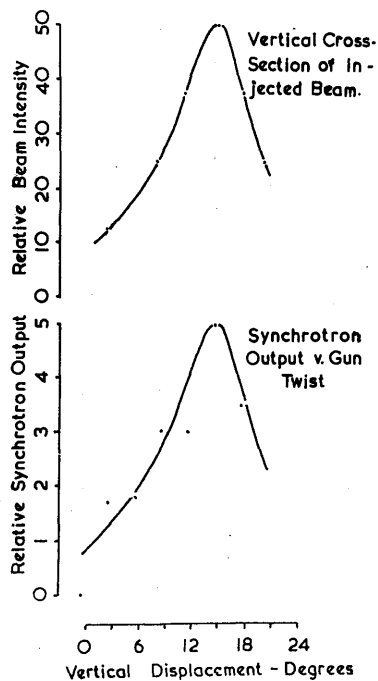


Fig 58 Calculated Injection Acceptance Angles



unexplained interference phenomenon involving the proximity of the stable limit to the resonator wall.)

In comparing the injection into the two machines it may therefore be submitted that while there is a certain case for using a relatively broad-beamed gun on the 30 MeV machine there can be no justification for a similar policy on the 300 MeV machine - unless it is based on an exaggeratedly pessimistic attitude to the problem of beam orientation relative to the gun body. The difference may also be approached from the point of view of space-charge, for it is clear that space-charge limitation plays a greater part in restricting the output of the small machine than it does in the case of the larger machine: this is indicated by the fact that 'good' and 'bad' guns have relatively little effect on the performance of the 30 MeV machine, whereas the output from the larger machine would seem to depend on little more than the peak electron intensity within the emission pattern, expressed relative to the overall emission.

Space-charge consideration have therefore been generally neglected; for insufficient work has been done on the smaller accelerator to derive useful

information, while in the more detailed work on the performance of the 300 MeV machine the shortcomings of a dispersed beam have tended to conceal the onset of such effects. It is not anticipated that that they will become the ultimate limiting factors on performance of the larger accelerator until the injection beam has been concentrated into an angle of about 0.5° or less in both cross-sections.

CONCLUSIONS

In summing up the achievements, implications, and potentialities of the work already undertaken, it is difficult to avoid being influenced by a large amount of general experience which it has not been possible to incorporate in this account. Some of that experience has certainly crystallized into a kind of working understanding which could probably have been clarified and given quantitative value if time and circumstances had allowed: much of it, on the other hand, has been of an essentially random nature and assumed importance, or still assumes importance, merely as tentative support for unconfirmed hypotheses. This general experience must now be taken into some account for it is difficult to give actual results and revealed potentialities their proper relative value without recognizing the extent to which matters of policy are affected by such accumulated knowledge.

The immediate results are the most easily collated. Central in importance is the gun testing unit, and this, it would appear, provides considerably greater flexibility and versatility than the various set-ups and temporary

installations used by manufacturers and other accelerator teams. Both the screen and probe techniques are still in a relatively primitive state of development and would benefit from considerable refinement, but it is doubtful if much change can be made without an appreciable amount of effort; quantitative rather than merely relative current density determinations might, however, be valuable, and probe improvement would therefore seem the more important.

From a purely operational standpoint - and since the electron gun plays such a large part in determining machine reliability it is a particularly important standpoint - the ability to test guns before installing them in accelerators has proved particularly useful.

The exposure of the shortcomings of the 100 kV type of gun may appear an essentially negative achievement, but it is nevertheless an important one; for the present gun and mounting are extremely well designed pieces of precision mechanical engineering which will not easily be replaced, however great may be the need for improvement. No serious effort has yet been made to rationalize the electron-optical aspects of the gun behaviour; but now that a method for reasonably accurate examination of

beam patterns has been developed, and more importantly, that a narrow injection beam has been shown essential to high output from the 300 MeV synchrotron, this would seem a particularly promising line for development. There may, in this direction, be some advantage in using a more elaborate type of gun, possibly of a multi-electrode nature, but such assemblies would involve corresponding multiplication of the high voltage supplies - tapped off the pulse transformer load, no doubt - and would need to be well justified before introducing the additional complexities of a multi-bushed gun. With an arrangement of this kind, however, it might be possible to shift the beam by non-mechanical means; but considerable additional development would probably be involved between producing a narrow beam and satisfactorily controlling its orientation by simple electrical means. For this reason it is important that a purely mechanical means of beam shifting should be developed. There seems no reason why the concentric sleeve arrangement of the present 100 kV guns could not be adapted in such a way that an electrode assembly mounted freely on a vertical axis within the inner sleeve might be tilted by the relative movement of the outer sleeve.

It is unfortunate that there is at present such a large discrepancy between the test unit ageing and the requirement set within the accelerator. (This work has only been done for the 300 MeV synchrotron, and no comparative information is at present available for the 30 MeV machine.) Much of this may be put down to the 5 p.p.s. vibrations imposed upon the gun in the accelerator when the magnet is being pulsed, but this only explains the discrepancy: it does not correct it. Correction is, however, a matter of importance, for there is no limitation to the flash-over current in the accelerator modulator, and the stored energy in the 5 microsecond delay-line is appreciably greater than in the test unit. Although it is indeed important that flash-overs should be avoided the means for higher voltage ageing may not be easily attained either. For the present limitation is set less by the modulator output voltage in the test unit than by the space-dictated clearances at which external flash-overs occur.

ALPHABETICAL REFERENCE LIST

- Adams G.D. 'A Method of Increasing Betatron Yield'
Review of Scientific Instruments 19,9 p607 1948
- Bohm D., and L. Foldy 'The Theory of the Synchrotron'
Physical Review 70 p249 1946
- British Standards Institution 'Rules for the Measurement
of Voltages with Sphere-Gaps' B.S. 358:1939
- Courant E.D. 'A Resonance Effect in a Synchrotron'
Journal of Applied Physics 20 p611 1949
- Elder F.R., R.V.Langmuir, and H.C.Pollock 'The Effect of
Vacuum Tube Size on X-ray Output of a
Synchrotron' Review of Scientific Instruments
19,2 p121 1948
- Fry D.W., J.W.Gallop, F.K.Goward, and J.Dain 'A 30 MeV
Synchrotron' Nature 161 p504 1948
- Goward F.K. 'The Effect of Azimuthal Inhomogeneities in
The Magnetic Field of a Betatron or
Synchrotron' Proceedings of the Physical
Society LXI p284 1948
- Kerst D.W. 'Acceleration of Electrons by Magnetic
Induction' Physical Review 58 p841 1940
'The Acceleration of Electrons by Magnetic
Induction' Physical Review 60 p47 1941
'A Method of Increasing Betatron Energy'
Physical Review 68 p233 1945
'A Process Aiding the Capture of Electrons
Injected into a Betatron' Physical Review
74 p503 1948
- Kerst D.W., and R Serber 'Electronic Orbits in the
Induction Accelerator' Physical Review
60 p53 1941
- Lawson J.D. 'The Effect of Doughnut Height and Gun Emission
on the Output of a Betatron' A.E.R.E. Memo
E1/M2 1949

Lawson J.D. 'Double Orbit in the 30 MeV Synchrotron'
Nature 165 p109 1950

Lempicki A., and A.B.MacFarlane 'Silicone Oil Vapour
and Secondary Electron Emission' Nature
167 p813 1951

MacFarlane F.W. et.al. Annulus Constriction Tests -
after Courant - Unpublished 1955

Westendorp J.A.P. 'The Use of Direct Current in Induction
Electron Accelerators' Journal of Applied
Physics 16 p657 1945

SEQUENTIAL FIGURE LIST

- 1 Schematic Diagram of Betatron
- 2 Glasgow 30 MeV Synchrotron
- 3 30 MeV Synchrotron Magnetization Curve
- 4 30 MeV Synchrotron n-value Curve
- 5 30 MeV Synchrotron Quadrature Flux Plot
- 6 30 MeV Synchrotron Loss Curve
- 7 30 MeV Synchrotron Betatron Gap Sensitivity
- 8 30 MeV Synchrotron Betatron Gap Geometry
- 9 30 MeV Synchrotron Tangential Field Plot
- 10 30 MeV Synchrotron Orbit Checking Circuit
- 11 30 MeV Synchrotron Output Sensitivity to Gap
- 12 30 MeV Synchrotron Betatron Characteristics
- 13 30 MeV Synchrotron Gun Dimensions
- 14 30 MeV Synchrotron First Gun Tilt Tests
- 15 Derived Results from Fig 14
- 16 30 MeV Synchrotron Gun Twist Test
- 17 30 MeV Synchrotron Second Gun Tilt Tests
- 18 30 MeV Synchrotron Output and 'n' at injection
- 19 30 MeV Synchrotron Third Gun Tilt Tests
- 20 The Complete Gun Testing Unit
- 21 Layout of the Gun Testing Unit

- 22 Test Chamber for 30 MeV Synchrotron Guns
- 23 Test Chamber for 300 MeV Synchrotron Guns.
- 24 The Complete 100 kV Modulator
- 25 Main Assemblies of the 100 kV Modulator
- 26 Circuit Diagram of the 100 kV Modulator
- 27 A Pulse-height Valve Voltmeter
- 28 Blackened Perspex-bound Screen
- 29 Life Test of a Silicate-bound Screen
- 30 The Fluorescent Screen Mounting
- 31 Photographic and Silicate Screen Linearities
- 32 Test Probe Geometry
- 33 Test Probe Aberration
- 34 Probe and Chamber Collection Linearity
- 35 Probe Unit Details
- 36 The Probe Unit Mounted on the Second Test Chamber
- 37 A Comparison of Data from Screen and Probe Tests
- 38 100 kV Pulse Transformer Measured Frequency Response
- 39 100 kV Pulse Transformer Calculated Pulse Response
- 40 100 kV Pulse Transformer Load and Divider
- 41 6.25cm Sphere-Gap
- 42 Injection Pulse Voltage Calibration
- 43 Gun Ageing Rate Curve
- 44 A 30 MeV Synchrotron Gun

- 45 A 300 MeV Synchrotron Gun
 - 46 Glasgow 300 MeV Synchrotron
 - 47 100 kV Gun Components
 - 48 100 kV Gun Test Mounting
 - 49 Gun Mounting on the 300 MeV Synchrotron
 - 50 Gun Mounting Components
 - 51 Beam Spread Measurements
 - 52 Derived Beam Spread Results
 - 53 Additional Anode Flange for 100 kV Gun
 - 54 Assembly Error in 100 kV Gun
 - 55 Tilt Analysis for 100 kV Gun
 - 56 Emission Contour Plot for 100 kV Gun
 - 57 Related Variation of Output with Gun Twist and Tilt
 - 58 Calculated Injection Acceptance Angles
 - 59 Second Contour Plot and Gun Twist and Tilt Test for
 100 kV Gun
-